Low-head pumped hydro storage: A review of applicable technologies for design, grid integration, control and modelling

Citation for the original published paper (version of record):
Hoffstaedt, J., Truijen, D., Fahlbeck, J. et al (2022). Low-head pumped hydro storage: A review of applicable technologies for design, grid
integration, control and modelling. Renewable and Sustainable Energy Reviews, 158.
http://dx.doi.org/10.1016/j.rser.2022.112119

Renewable and Sustainable Energy Reviews 158 (2022) 112119

Contents lists available at ScienceDirect

Renewable and Sustainable Energy Reviews

journal homepage: www.elsevier.com/locate/rser

Low-head pumped hydro storage: A review of applicable technologies for design, grid integration, control and modelling

J.P. Hoffstaedt [a,*], D.P.K. Truijen [b], J. Fahlbeck [c], L.H.A. Gans [d], M. Qudaih [e], A.J. Laguna [a], J.D.M. De Kooning [b], K. Stockman [b], H. Nilsson [c], P.-T. Storli [d], B. Engel [e], M. Marence [f], J.D. Bricker [g,h]

[a] Faculty of Mechanical, Maritime and Materials Engineering, Department of Maritime and Transport Technology, Delft University of Technology, Mekelweg 2, 2628 CD Delft, The Netherlands
[b] Department of Electromechanical Systems & Metal Engineering, Ghent University & FlandersMake@UGent - Corelab EEDT-MP, Sint-Martens-Latemlaan 2B, 8500 Kortrijk, Belgium
[c] Department of Mechanics and Maritime Sciences, Division of Fluid Dynamics, Chalmers University of Technology, 412 96 Gothenburg, Sweden
[d] Department of Energy and Process Engineering, Waterpower Laboratory, Norwegian University of Science and Technology, NO-7491 Trondheim, Norway
[e] Elenia Institute for High Voltage Technology and Power Systems, Technische Universität Braunschweig, Schleinitzstraße 23, 38106 Braunschweig, Germany
[f] IHE Delft Institute for Water Education, Westvest 7, 2611 AX Delft, The Netherlands
[g] Department of Hydraulic Engineering, Hydraulic Structures and Flood Risk, Delft University of Technology, The Netherlands
[h] Department of Civil and Environmental Engineering, University of Michigan, 2350 Hayward, Ann Arbor, MI 48109-2125, USA

ARTICLE INFO

Keywords:
Low-head pumped hydro storage
Energy storage
Grid stability
Renewables integration
Energy transition
Reversible pump-turbine

ABSTRACT

To counteract a potential reduction in grid stability caused by a rapidly growing share of intermittent renewable energy sources within our electrical grids, large scale deployment of energy storage will become indispensable. Pumped hydro storage is widely regarded as the most cost-effective option for this. However, its application is traditionally limited to certain topographic features. Expanding its operating range to low-head scenarios could unlock the potential of widespread deployment in regions where so far it has not yet been feasible. This review aims at giving a multi-disciplinary insight on technologies that are applicable for low-head (2-30 m) pumped hydro storage, in terms of design, grid integration, control, and modelling. A general overview and the historical development of pumped hydro storage are presented and trends for further innovation and a shift towards application in low-head scenarios are identified. Key drivers for future deployment and the technological and economic challenges to do so are discussed. Based on these challenges, technologies in the field of pumped hydro storage are reviewed and specifically analysed regarding their fitness for low-head application. This is done for pump and turbine design and configuration, electric machines and control, as well as modelling. Further aspects regarding grid integration are discussed. Among conventional machines, it is found that, for high-flow low-head application, axial flow pump-turbines with variable speed drives are the most suitable. Machines such as Archimedes screws, counter-rotating and rotary positive displacement reversible pump-turbines have potential to emerge as innovative solutions. Coupled axial flux permanent magnet synchronous motor-generators are the most promising electric machines. To ensure grid stability, grid-forming control alongside bulk energy storage with capabilities of providing synthetic inertia next to other ancillary services are required.

Abbreviations: ADRC, Active Distribution Rejection Control; AF-PMSM, Axial Flux Permanent Magnet Synchronous Machine; ANN, Artificial Neural Network; AS, Ancillary Services; CAES, Compressed Air Energy Storage; CRPT, Counter-Rotating Pump-Turbine; DSO, Distribution System Operator; DSSR, Double-Stator Single-Rotor; DTC, Direct Torque Control; EIA, Energy Information Administration; ESHA, European Small Hydropower Association; ESOEI, Energy Storage On Energy Invested; ESS, Energy Storage System; FOC, Field Oriented Control; IRES, Intermittent Renewable Energy Source; LCOS, Levelised Cost Of Storage; MEPT, Maximum Efficiency Point Tracking; MMD, Modular Machine Drive; MPC, Model Predictive Control; MPPT, Maximum Power Point Tracking; MTPA, Maximum Torque Per Ampere; PAT, Pump As Turbine; PHS, Pumped Hydro Storage; PLL, Phase Locked Loop; PM, Permanent Magnet; PMSM, Permanent Magnet Synchronous Machine; PTO, Power Take-Off; PWM, Pulse-Width Modulation; RPT, Reversible Pump-Turbine; SSDR, Single-Stator Double-Rotor; SSSR, Single-Stator Single-Rotor; SVM, Space Vector Modulation; TSO, Transmission System Operator

* Corresponding author.
E-mail address: J.P.Hoffstaedt@tudelft.nl (J.P. Hoffstaedt).

https://doi.org/10.1016/j.rser.2022.112119
Received 8 September 2021; Received in revised form 17 December 2021; Accepted 9 January 2022

1. Introduction

In a global effort to reduce greenhouse gas emissions, renewables are now the second biggest contributor to the world-wide electricity mix, claiming a total share of 29% in 2020 [1]. Although hydropower takes the largest share within that mix of renewables, solar photovoltaics and wind generation experience steep average annual growth rates of 36.5% and 23%, respectively, since 1990 [2]. Both of these technologies, however, significantly differ in their generation characteristics when compared to traditional thermal power plants. This trend towards an increase in intermittent generation, coupled with a reduction in spinning reserves, could undermine grid stability. To counteract these effects, grid-scale deployment of energy storage is indispensable.

There are complementary approaches to balance demand and supply in an electricity grid, such as an increase in flexible generation, demand management, or exporting and importing electricity. Nonetheless, at certain penetration levels of renewables, to reduce the risk of grid instability, a heterogeneous pool of storage solutions is needed. A wide variety of such storage technologies – including capacitors, flywheels, electro-chemical batteries, compressed air energy storage (CAES), molten-salt or hydrogen storage – is available to balance the grid in the timescale from seconds up to seasonal variations. Crucial factors for large-scale balancing include energy and power capacity as well as fast response times while maintaining high efficiencies. Aside from fulfilling these criteria, the major driver towards commercial deployment is the levelised cost of storage (LCOS); leading in this are pumped hydro storage (PHS) and CAES [3]. An alternative approach is based on the so-called energy stored on energy invested (ESOEI), which gives an estimate of the relation between the stored energy during the lifetime of a system and the energy required to construct the system. Also for this metric, PHS and CAES are, by far, in the lead [4].

Pumped hydro storage is a mature and well-known technology that has been used since the beginning of the 20th century. In 2020, it contributed with 90.3% of the world's energy storage capacity [5]. However, while some regions reach the limits of economically viable PHS that can be implemented, others lack entirely the necessary topographic features. Traditional PHS relies on high heads to realise the expected power and storage capacity. Most of the plants produce in the order of 1000–1500 MW of power, with round-trip efficiencies which are commonly in the range of 70%–85% [6].

Aside from its use to store energy, hydropower is regarded as the foremost renewable generation method when it comes to flexibility and improving grid stability. Due to the proven advantages of hydroelectric power generation, wide-ranging research efforts have focused on conceptual adaptations and technological advancements utilising low- and ultra-low-head scenarios. Some of these technologies, such as wastewater, run-of-river hydropower, or tidal barrages have seen prototyping and commercial deployment. However, theoretical attention and practical implementation towards low-head PHS has been limited. Fig. 1 shows a conceptual drawing of what such a system may consist of when deploying a reversible pump-turbine coupled to a motor-generator that is connected to the grid via an AC-DC-AC converter for variable speed operation.

The lack of attention on low-head PHS can be partly explained through high levelised cost of storage (LCOS) caused by extensive civil structures, enlarged machinery, lower round-trip efficiencies, and limited flexibility to provide ancillary services (AS). The predicted increase in demand for energy balancing and AS in the upcoming decades will likely justify increased LCOS. Additionally, technological advancements could significantly contribute to a reduction in LCOS. Addressing the technological challenges and overcoming economic barriers of low-head PHS could unlock the potential of integrating large-scale energy storage into the grids of regions where it has not been feasible so far.

For the given reasons, research and development towards shifting the operating range of PHS to low heads is scarce. Using a multi-disciplinary approach, the main goal of this research is to review and analyse technologies based on their applicability for low-head utilisation. First, an overview of PHS and its historical development is given. Based on this, recent trends leading to further innovation in the field are identified, and the potential and necessity of storage technologies are discussed. Finally, technological and economic challenges are explored, and the key advancements that could contribute to economic and technical viability are isolated. Building on this, in the major technological fields – pump-turbine design and configuration, control and electric machinery, as well as modelling – the most promising technologies are compared and their fitness for low-head application is assessed. Additionally, implications of grid integration are discussed, including further elaboration on the significance of integrating large-scale energy storage, such as low-head PHS into world-wide grids.

2. Overview and historical development of pumped hydro storage

Pumped hydro storage is an amended concept to conventional hydropower as it cannot only extract, but also store energy. This is achieved by converting electrical to potential energy and vice versa in the form of pumping and releasing water between a lower and a higher reservoir. The energy conversion occurs by using pumps and turbines either combined in a reversible (binary set) or separate configuration (ternary and quaternary sets). The power of such a system, as well as the amount of energy that can be extracted or stored, is proportional to the product of head and water flow or volume, respectively. Hence, a higher head results in a reduced flow for a given desired power and smaller reservoirs for a given storage capacity. It does not, therefore just correlate with scaled-down reservoirs but also smaller remaining civil structures and machinery, historically leading to reduced cost and a significant economic advantage of utilising high-head differences [7].

Of today's bulk energy storage integrated into the world-wide grids, over 90% is comprised of PHS of which the vast majority are high-head applications. According to the International Hydropower Association, in 2019, the global installed capacity reached 158 GW with the biggest contributors being China making up 30.3 GW of the share, Japan 27.6 GW, and the United States 22.9 GW [8]. Fig. 2 shows the distribution of global storage capacity that is operational, under construction, planned, and announced as of 2021.

In comparison, the next largest contributors to bulk energy storage are electro-chemical battery storage – rapidly growing with a total capacity of 14.2 GW – and thermal storage with 2.9 GW in 2020 [5]. To explain the historic market dominance of PHS and understand recent trends, several factors have to be taken into account. Pumped hydro storage utilising reversible pump-turbines has been available as a mature and cost-effective solution for the better part of a century with an estimated energy based capital cost of 5–100 $/kWh [10]. Today, compressed air energy storage is considered mature and reliable, offering similarly low capital cost between 2–50 $/kWh, and electro-chemical batteries offer high energy density with higher costs, and experience drastic growth while the impact of hydrogen-based storage in the energy transition is largely expected to be substantial [10].

However, PHS‘s dominance is not only due to its historic lead but can also be attributed to its technical, economic, and sustainability advantages. These include high efficiencies, large achievable capacities, and long lifetimes. Compared to rapidly expanding battery storage that can be used wherever it is most needed, one clear advantage is this durability. It is currently assumed that a battery system will last around 15–20 years, but on the other hand, the oldest hydropower plant in Norway has been operating for over 120 years [11,12]. Prolonged lifetimes are one factor improving the sustainability of PHS compared to other storage solutions. Others include maturity, low capital and operating cost, as well as low energy and carbon dioxide density. Based on these and other factors regarding economic, performance, technological, and environmental considerations, Ren et al. ranked PHS as the most sustainable storage technology [13].

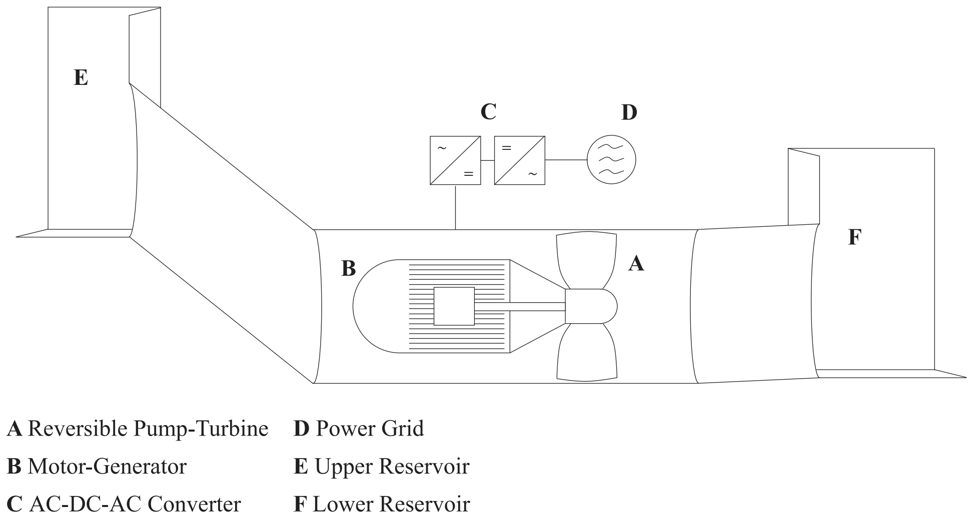

Fig. 1. Schematic showing a low-Head PHS concept and its main components.

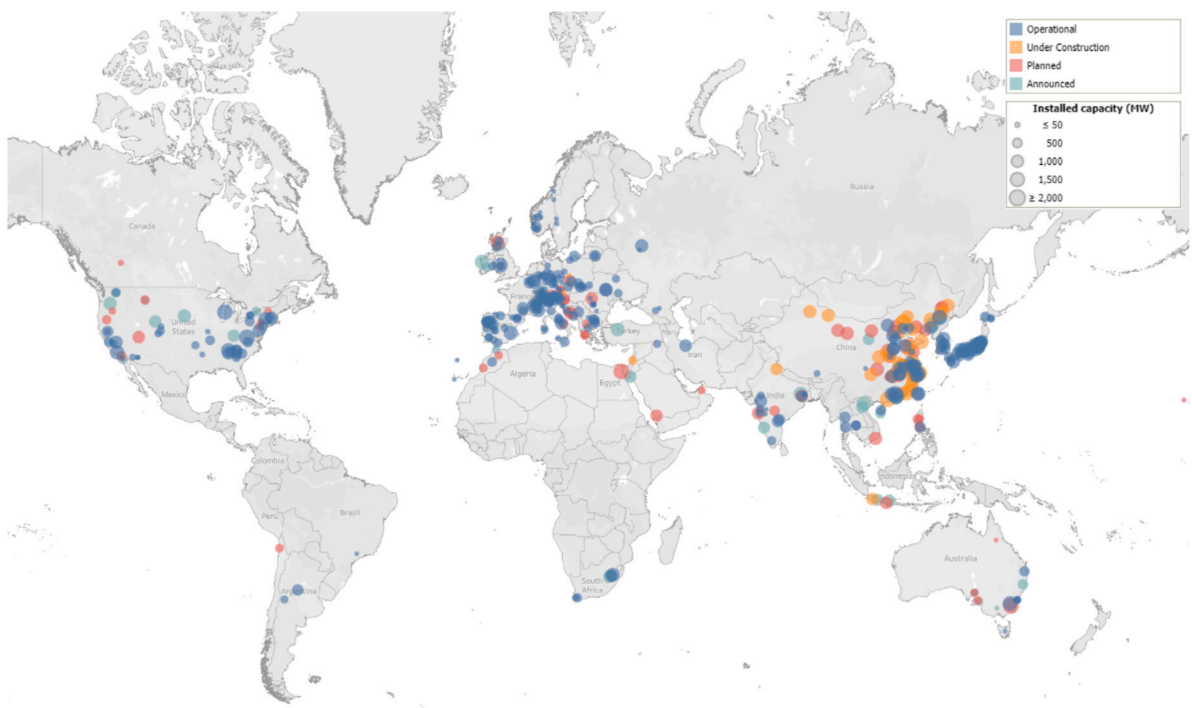

Fig. 2. Global PHS Capacity [9].

Further advantages of PHS include suitability for long-term storage – since hardly any storage losses occur other than seepage and evaporation – and quick availability due to short switch-on and switch-off times. With these factors ensuring a significant share within a heterogeneous pool of storage technologies, one major disadvantage of PHS has historically been its topographic constraints. A switch from river-based to closed-loop off-river systems could overcome some of the constraints and increase the potential for deployment [14,15]. Nonetheless, regions with flat topographies still do not offer viable sites.

2.1. Early deployment and progression in the **20***th century*

Not long after hydropower began to generate electricity, the first small-scale PHS plants were constructed in the mountainous regions of central Europe in the beginning of the 20th century. Initially using separate pumps and turbines, combined reversible pump-turbines have become the norm since the middle of the 20th century [6]. Experiencing a major boom in Europe, parts of Asia, and North America, a large portion of today‘s installed PHS capacity was constructed in the 1960s, 1970s, and 1980s; in most countries, this occurred alongside rapidly increasing nuclear power. The gained flexibility that PHS plants provided allowed them to match a varying demand with the baseload generation of nuclear power plants. An example where this was particularly relevant is Japan due to its lack of interconnections to other countries as well as their strong strategy towards nuclear energy.

In the United States, another reason for the growing capacity of PHS during that period was the energy crisis in the 1970s, leading to an increased cost of fossil fuels allowing PHS to grow as a substitute for peak balancing [16]. After that period, development slowed down in most regions with the major exception of China. Its rapidly growing economy and correlated energy demand largely satisfied by non-flexible coal plants required major energy storage.

Up until this point, pump-turbines were coupled to fixed speed motor-generators. The next significant development occurred in the 1990s when variable speed operation was introduced in Japan. The ability to adjust the angular velocity of the runners allowed for higher efficiencies under changing conditions, reduced the switching time between pump and turbine mode, and facilitated higher ramp rates and quicker response times [17].

2.2. Recent trends

After an initial reduction of PHS deployment around the turn of the millennium, the rapidly growing share of intermittent renewable energy sources (IRES) in the last couple of decades sparked new interest in sustainable flexible generation as well as large-scale energy storage solutions. This caused increasing attention towards the rehabilitation of old hydropower plants and an expansion of PHS [18]. While PHS experienced a much longer development process than competitive technologies and could hence be considered mature, two major trends can be identified pushing further innovation in the field.

The first one is derived from the change in grid characteristics caused by a reduction in spinning reserves. A growing number of converter coupled renewables raise the necessity for external provision of AS. To provide these using PHS, research efforts focus on developing improved control and machinery but also novel concepts, such as hybrid storage solutions. Examples of such concepts could be the coupling of conventional PHS with flywheels for frequency control or supercapacitors providing virtual inertia [19]. Hybrid storage solutions incorporating PHS, such as hybrid pumped and battery storage, are also particularly suited for off-grid applications [20].

The second major trend is expanding the operating range and application. One of the most limiting factors in the potential use of large-scale PHS has been the fact that not many locations could offer economically viable deployment. These were traditionally mountainous regions accessing water with enough space to construct extensive civil structures. There is a large potential in Europe to deploy further mini and small hydropower plants to counteract the effects of higher renewable penetration levels. However, this does not apply to countries with flat topographies, such as Denmark, the Netherlands, or Belgium [21]. Additionally, to achieve the balancing capabilities of pumped storage systems, larger plants typically provide better economies of scale. Suitable locations for such are rare in Europe and some countries like Japan are considered to have used nearly all available sites [22]. This limited availability of appropriate locations drives the development of new approaches. Examples for a promising change of approach are underwater PHS or gravity energy storage.

The former is a recently developed and tested concept based on submerging a hollow sphere offshore and using the static pressure difference for energy storage. The surrounding sea acts as the upper reservoir and the sphere as the lower which can be filled to generate electricity or emptied to store it. Initial model-scale tests have been successful; it is a freely scalable technology without issues regarding land use and considered cost competitive with PHS and compressed air storage [23]. Using seawater in general for PHS is so far an uncommon practice, but has been investigated as a solution for isolated grids [24]. If technical, environmental, and economic challenges are overcome, utilising seawater could be another promising expansion of PHS's potential deployment.

The latter similarly decouples the fundamental principle of PHS from its topographic restrictions. Storage is done via gravitational potential energy. However, energy is stored or extracted respectively by moving a piston of large mass up and down using water powered by a pump-turbine for conversion. While still under development, initial economic evaluations show it to have a potentially attractive LCOS compared to other storage technologies [25].

An alternative that is not less promising and will potentially suit both these trends is to extend the operating range of conventional PHS to low and ultra low-head applications, including the potential use of seawater, while improving its capability to provide AS. If technological advancements allow for economic viability, large-scale low-head PHS could be integrated in regions where PHS so far was not a feasible solution.

Later trends for PHS show the usage of ternary units. With ternary units, a separate pump and turbine are connected on a single shaft to an electric machine that can work either as a motor or a generator [26]. This configuration presents a very flexible and fast response range, shows higher efficiencies than reversible machines, and can utilise hydraulic short circuits for optimal power in- or outtake [27,28]. The major drawback with ternary units is that they requires higher investment and maintenance costs compared to a reversible unit [28]. In a low-head scenario, the increase in investment cost would be even greater since a high-power, low-head machine needs to be large in order to handle a high flow rate. Thus, it is suggested as a less attractive alternative for low-head PHS.

2.3. Potential of deployment and scalability in Europe

Resulting from the rapid transition that grids are experiencing worldwide, the need for energy storage is evident. However, there are a variety of factors influencing the actual storage demand and its expected progression during the coming decades. First and foremost, this is the growth in intermittent and converter coupled renewables. While a direct correlation between renewable penetration levels and storage demand can be assumed, mitigating factors such as improved generation forecasting and the continuous development of renewables able to provide AS will allow for later deployment of energy storage. Further factors to consider include the flexibility of remaining generators in the grids and the emerging need for additional operating reserves, improved demand management, as well as further grid expansion and interconnection.

Bearing these factors in mind, it becomes clear that storage demand will heavily depend on individual grid characteristics and may vary in different regions. Based on Germany as an example, additional short-term storage can be expected at renewable shares between 40% and 60% and long-term storage between 60% and 80%. Above 80% and towards a fully renewable generation, bulk energy storage on all timescales is not only required in order to avoid extensive renewable energy curtailing, ensure grid stability and power quality, but will be a cost-effective solution in the GW range [29]. In less flexible grids, for example utilising large-scale nuclear power to cover the base load, the need for extensive storage will be reached at much lower renewable levels.

An update to the European Green Deal has raised the ambition to reduce greenhouse gas emission by 55% until 2030 compared to the standard of 1990 paving the way for a carbon neutral energy supply by 2050. Consequently, the share of intermittent renewables will need to increase faster. Recent estimates see a growth towards 70% renewable power generation in 2030 [30].

Depending on the flexibility of this share of renewables in different regions, a rapid increase in demand for storage and the provision of AS can be expected with PHS being a promising candidate to fill the gap. For countries with a flat topography, economically viable low-head PHS could bear a huge potential to cover the growing demand. This is especially relevant if a large coastline is available, opening up the possibility for seawater application. Coastal applications also come with the additional benefit of proximity to large-scale IRES, such as offshore wind farms.

2.4. Technological and economic challenges

Low-head PHS has not yet seen deployment on a significant scale within our grids. This is largely due to the increased upfront cost required. While highly dependent on the individual project and site, the major contributor to the initial CAPEX of PHS projects in general are civil structures, including the reservoir, penstock, and lining [31]. Due to larger masses of water being stored in the reservoir and flowing through the penstock when it comes to low-head applications, their contribution to the overall economic viability can only be assumed to be significant. All aspects regarding civil components as well as detailed economic analyses of low-head PHS systems are, however, outside of the scope of this review.

Low-head PHS would be most competitive utilising a storage capacity able to provide balancing in the timescale of hours to days. This places it in the middle between lithium-ion batteries appropriate for shorter and hydrogen storage appropriate for longer periods. The LCOS of new high-head PHS systems ranges from 50 €/MWh to 80 €/MWh [32]. Initially low-head plants may not be able to compete with this. However, changing demand characteristics of the electricity markets, as well as further development and improvement of technological aspects, significantly influence economic viability and thereby the potential of large-scale deployment. The increase in renewables in world-wide grids will lead to rising demands, not just for short- and long-term balancing but also the provision of AS increasing the value of both. Additional revenue from the provision AS could hence increase economic viability.

Further drivers making PHS economically more attractive are growing interconnections to other grids opening up additional markets as well as technical advances such as higher efficiencies across a broader operating range [22]. Technological progression can help facilitate these drivers. A reduction of switching times between pump and turbine mode together with higher power ramp rates will allow for enhanced capabilities to provide AS as well as maximise balancing. Aside from regulatory changes, such as carbon taxation, electricity price margins have been identified as one of the major drivers towards PHS utilisation. Improved round-trip efficiencies directly correlate with higher revenues for the operator and therefore result in increased utilisation [33].

Based on these challenges, three main areas can be identified where significant progress could contribute to making low-head PHS technically and economically competitive. These are pump-turbine design and configuration, grid integration, and electrical machines and control. Research in these fields will be discussed in the chapters following. Additionally, modelling approaches that may aid the development are compared.

3. Pump-turbine design and configuration for low-head pumped hydro storage

The choices when selecting the type of reversible pump-turbine (RPT) unit, or evaluating using a pump as turbine (PAT), are governed by a number of factors. The first thing to evaluate is the power of the hydropower plant, which is a function of head and flow rate and the general formula is given by Eq. (1).

$$P = \rho g H Q \eta \tag{1}$$

Here, ρ is the density of water, g is the gravity acceleration, H is the head, Q is the volumetric flow rate, and η is the overall efficiency of the power plant. The gravity acceleration and water density can be regarded as constant. The equation shows that if the head is low, the flow rate must be large in order to produce high power [34]. With a large flow rate, the diameter of pipelines and the runner need to be large as well to limit the flow velocity, and thus hydraulic losses in the system. High-head conditions are usually preferable to build pump storage hydropower plants. However, low-head solutions with high volumetric flow rate are also regarded as having great potential to unleash new opportunities for pumped hydro storage [35].

The definition of low-head is not unanimous among different countries and researchers. For example, the U.S. Energy Information Administration (EIA) considers low-head when the head is less than 30 metre and Okot [36] classifies it as when $5 < H < 15$ metre. In this work, the European Small Hydropower Association (ESHA) classification defines low-head, and states that low-head hydropower plants have a head of 2-30 metre [37].

The overall efficiency of a low-head power plant is more sensitive to head losses than a high-head alternative, and low-head PHS requires that the pipelines are short to be economically feasible [38]. This is because head losses are proportional to the pipeline length and the flow velocity squared, which is a further incentive for not using ternary units in a low-head case since they require more pipelines and would thus decrease the plant‘s overall efficiency. With the higher flow rate of high-power low-head PHS, larger reservoirs are required to store the same amount of energy as a corresponding high-head application [34]. This is because the energy storage capacity is a function of the water mass and head. Apart from that, other conditions such as the type of machine (radial-, mixed-, or axial-flow), operation (variable or fixed speed), and reservoir configuration may apply when choosing the best reversible pump-turbine configuration [39]. Chapallaz et al. [40] stated that, in practice, almost any hydro pump can also be used as a turbine. The reverse is, however, not the case. As an example, impulse turbines (Pelton or Turgo) cannot be used as pumps.

The design and characteristics of any hydro pump and turbine are determined by its conditions of operation. In turbomachinery, the specific speed is one key parameter to select the most appropriate reversible pump-turbine or using a pump as turbine (PAT). In this paper, it is defined in accordance with Dixon and Hall [41] as Eq. (2), and Table 1 shows ranges of specific speeds for various machines.

$$\Omega_s = \frac{\Omega Q^{1/2}}{(gH)^{3/4}} \tag{2}$$

Here, Ω is the runner rotational speed in rad/s, Q is the volumetric flow rate in m^3/s, and H is the head in metre. Stepanoff [42] explained in 1948 that a higher specific speed results in a smaller, and thus cheaper, machine. With a higher flow rate, the blade design differs significantly, as illustrated in Fig. 3. On the other hand, machines with low rotational speeds and small shear forces (e.g. Archimedes screw and positive displacement machines) are more fish-friendly [43,44]. Radial- or mixed-flow machines are preferable for pumps with a specific speed of $\Omega_s < 2.7$, and as the specific speed increases ($2.6 < \Omega_s < 11.6$), an axial configuration is more suitable [45].

Carravetta et al. [46] postulate that axial-flow pumps can be used as PAT for heads between 1–5 m and flow rates up to 1000 l/s. They also claim that mixed-flow PATs can be used for heads in the region of 5–15 m and flow rates of 50–150 l/s. Bogenrieder [47] stated that radial pump-turbines are suitable to use for heads that are above 60 metre, with a power exceeding 50 MW. Typically, radial- or mixed-flow machines work best for high heads and low flow rates. For example, regular Francis-like pump-turbines (mixed-flow) are the common choice when it comes to mid- to high-head applications, but the head variations at low-head operation would greatly affect efficiency [48]. Mixed-flow machines can be used as low-head PHS if the flow rate is low. However, according to Eq. (1), this implies that the power will also be low. Multiple machines could be used in parallel to increase the total power. Breeze [48] suggests that a Deriaz, mixed-flow machine can be used for heads between 20–100 m. This is because its design is closer to an axial machine compared to a conventional Francis-like pump-turbine and the Deriaz design also presents adjustable blades [48,49]. Breeze further expresses the necessity of variable speed drives to extend the operational region at high efficiency.

The reason why an axial machine is preferable in a low-head application is that it allows for a higher flow rate, which is necessary

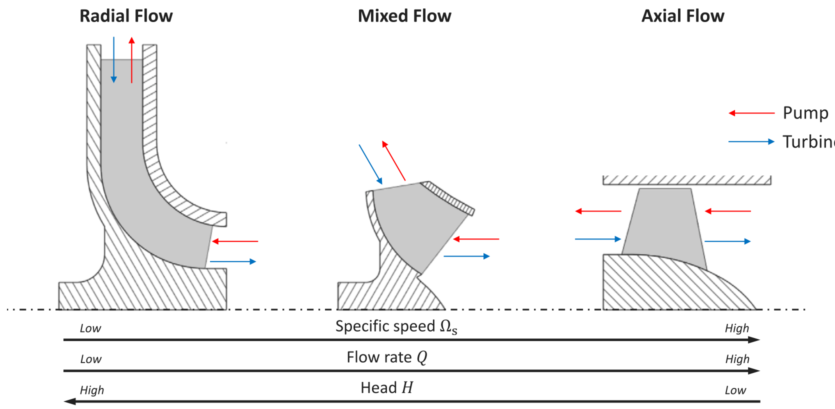

Fig. 3. Principle view of bladed pump-turbine configurations, note that the term “centrifugal” refers to both the radial- and mixed-flow. The drawing is based on principles shown in [40–42,46].

Table 1
Ranges of specific speed for various machines [45].

Technology	Specific speed Ω_s
Axial[a]	2.6–11.6
Mixed	0.6–2.7
Radial	0.1–0.8
Archimedes screw[b]	0.03–0.39
Positive displacement[b]	0.01–0.13

[a]CRPT is classified as an axial machine.
[b]Values should be regarded only as a reference number, since it is not common to indicate a specific speed for these machines.

for a machine with high power at low heads. An axial machine also allows for cheaper civil structures. In turbine mode, the runner rotates due to the torque that is generated by the flow-induced runner blade pressure and suction sides. The electric generator extracts power by a balancing counteracting torque at the particular rotational speed. In pump mode, an electric motor adds power to the runner in the form of torque at the particular rotational speed. A flow is developed due to the rotating runner blade pressure and suction sides, causing a balancing counteracting torque. The pressure change is in an axial machine primarily due to the change of relative flow velocity [45]. This is because the tangential velocity of the runner and the cross-sectional area are constant along a streamline in an axial machine. In a centrifugal machine, the flow must change direction from axial to radial (pump mode), or radial to axial (turbine mode), as shown in Fig. 3. The principles for the head rise in a centrifugal machine are here described in pump mode for brevity. As the flow goes through the machine, the cross-sectional area and the tangential velocity of the runner increase with the radius through the machine. The absolute flow velocity will decrease as the cross-sectional area increases, due to continuity. According to Bernoulli’s principle, the static pressure will increase with the change of absolute velocity squared [50]. The main cause of the static pressure rise is, however, due to centrifugal effects caused by the increase of the runner’s tangential velocity, and passage diffusion, due to a reduction in the relative flow velocity, through the machine [45]. The result is that the exit blade velocity needs to be small in order to limit the pressure rise in a low-head application. This means that the machine needs to be small and that the entrance-to-exit diameters decrease with the decreasing head [51]. The smaller size further limits the flow rate and thus the power.

In general, pump-turbines are worse at part-load conditions compared to a pure pump or turbine since the pump-turbine design is often a trade-off to reach acceptable performance at design conditions [52,53]. Delgado et al. [54] reported that it is hard to predict part-load performance for PATs, especially in turbine mode since pump manufacturers usually do not supply any data of this. Stepanoff [42] stated that centrifugal machines have preferable efficiency as a function of flow rate; however, axial machines have a flatter efficiency curve as a function of head. This further suggests that an axial machine is preferable in a low-head scenario due to the fact that part-load operations will be less influenced by the large variation in head of a low-head PHS application.

Lately, axial-flow pump-turbines with two runners, rotating in opposite direction from one another, have been proposed as an alternative for low-head PHS. They are usually referred to as counter-rotating pump-turbines (CRPT) due to the rotation of the individual runners, as illustrated in Fig. 4. According to Furukawa [55], the advantages of those machines are that they can be of smaller size, have a more stable head-flow rate characteristic curve, and have a wider range of high efficiency with individual speed control of the runners when compared to a single runner axial machine. Several numerical studies predict that a well designed low-head counter-rotating pump-turbine may achieve efficiencies of up to 80%–90% in both pump and turbine mode [56–58]. Fahlbeck et al. [59] showed numerical results for a prototype counter-rotating pump-turbine in pump mode with a peak efficiency of 91%, heads up to 12 metre, flow rates between 60–160 m^3/s, and a maximum power of almost 14 MW.

Additional non-conventional machines have also been studied as low-head PHS. The Archimedes screw, depicted in Fig. 4, is a viable option for heads between 2–10 m, discharge ranges up to 15 m^3/s, and power output of up to 355 kW [36,43,60]. The Archimedes screw enables lower installation and maintenance costs compared to other conventional pump-turbines and can reach efficiencies of up to 90% in turbine mode [61,62]. An additional benefit is that the Archimedes screw presents better conditions for fish-friendliness when compared to conventional bladed pump-turbines [43,61,63].

Positive displacement (PD) pumps are usually chosen when the system requires low specific speeds [45]. Some PD pumps can also represent a good alternative when reversible flows must be taken into account, thus resembling a PAT [64]. Positive displacement pumps are self-priming, typically produce low flow rates, can handle big variations in head without significantly changing their efficiency, and are often regarded as a good choice for viscous fluids or fluids with the presence of solids or precipitates that need to be handled [45,50]. Rotary positive displacement machines have already been studied as micro hydro turbines in water supply pipelines with pressures up to 5 bar (hydraulic head equivalent to 51 metre) and presented efficiencies between 60%–80% [65–68]. From all the available PD alternatives, the lobe and gear pump configurations – illustrated in Fig. 4 – are the most suitable options to handle reversible flow. Given the low specific speed, PD pumps could most likely be regarded as a fish-friendly technology [44]. On the other hand, only the lobe design seems to handle fish and solid without extra mitigation measures. A few small-scale projects have tested PD RPTs [64]. However, further investigations and real-scale

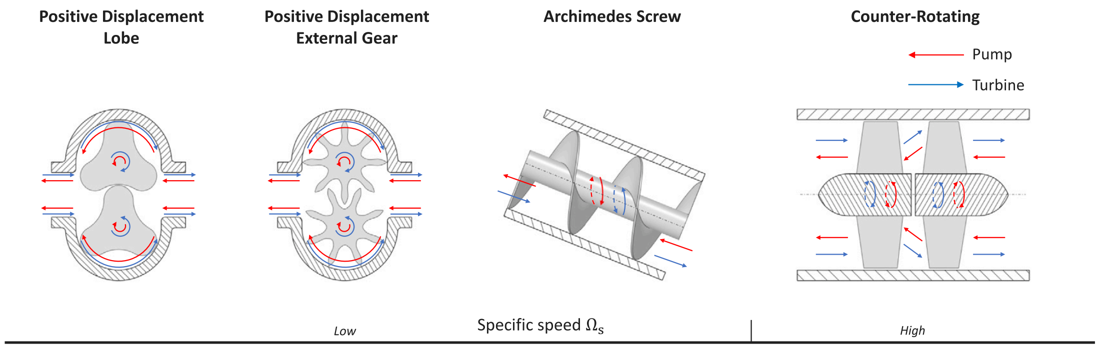

Fig. 4. Principle view of non-conventional pump-turbine configurations. The drawing is based on principles showed in [45,55,56].

prototypes are still needed to validate the use of PD RPTs in low-head pumped storage application.

Pump-turbines in PHS applications can operate at fixed or variable rotational speed. Variable speed machines take advantage of a wider operating range at high efficiency and can thus produce power in a wider spectrum [38,69]. Moreover, variable speed units ensure greater penetration and bring more flexibility to PHS operations, especially for smaller machines [70]. Despite the technical advantages, this technology is about 30% more expensive than fixed speed units. Thus, the choice between the two speed control options relies on both techno-economic and demand aspects [38,70].

4. Grid integration of energy storage systems

A reliable electrical power grid is a balanced system. As generation and demand fluctuate perpetually, transmission system operators (TSO) and distribution system operators (DSO) have to keep the system balance everywhere in the electrical grid. This balance ensures that the grid operates at its nominal frequency (50 or 60 Hz) and that voltage and power load remain within a certain limit at all times. However, the higher the penetration of intermittent renewable energy sources, the more insecure this balance. Thus, the increasing penetration of IRES is a challenge that TSO and DSO have to handle [71,72].

At the present time, power systems rely on conventional power plants utilising synchronous generators contributing significantly to the stabilisation of the electrical power system, using the rotating masses in their generators (rotors). The synchronous generators keep the frequency steady at its nominal value due to their large flywheel masses and thereby assure system stability. In the case of generation or load fluctuation leading to sudden grid frequency deviations, the rotor's combined inertia keeps the generators rotating and consequently supports the grid stability [73]. On the contrary, not all IRES have large rotating masses and most are integrated into the grid via converters, subsequently decoupling the rotating masses from the grid frequency. Therefore, they do not have any natural inertia (spinning reserve) and thus operate in an entirely different way than synchronous generators. As of today, the grid-connected converters for IRES follow the grid frequency by using a phase locked loop (PLL). This tracks the grid frequency in order to keep the IRES converters synchronised to the grid. The PLL control concept is known as grid-following control [73,74].

To tackle the challenge of increasing IRES and decreasing natural system inertia without affecting the system stability, two approaches are feasible. The first is to maintain a minimum number of rotating machines. Among other purposes, the contribution of short-circuit power and voltage support can provide the necessary inertia to the transmission system in a case of disturbances in the grid [75,76]. The second solution is through IRES itself. This occurs by using the capabilities of the power electronics, or energy storage systems (ESS), to provide and ensure a stable grid frequency without any synchronous rotating machines. For this purpose, a grid-forming control mode is currently being developed and tested in many research projects. Here, the

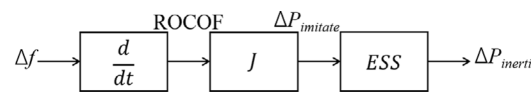

Fig. 5. Simplified block diagram for synthetic electrical inertia control [80,81]. Here, Δf is the deviation of system frequency, ROCOF is the rate of change of frequency, J is the virtual inertia control constant, $\Delta P_{\mathrm{imitate}}$ is the active power of the converter, and $\Delta P_{\mathrm{inertia}}$ is the emulated virtual inertia power that could be imitated into the system.

controlled converter acts as an AC voltage source with stated voltage, phase, and frequency. By controlling the voltage magnitude and frequency, the converter behaves very similar to a synchronous generator. The fundamental difference between grid-following and grid-forming is the way of synchronisation. By applying the swing Eqs. (3) and (4) [77], the grid-forming control strategy calculates the voltage angle and amplitude deviation, using current power transfer. It is thus self-synchronising. Therefore, a converter using grid-forming control coupled with an ESS is currently being discussed as a viable alternative to imitate the synchronous generator's behaviour regarding frequency control, especially its ability to provide synthetic electrical inertia [73,74,78]. In power plants with rotating mass and consequent inertia that are decoupled from the grid frequency, an additional control loop is required that gives a power reference proportional to the derivative of grid frequency. To provide the additional power requested by the synthetic inertia, the plant may still rely on the physical inertia present but due to its decoupled nature depends on said synthetic inertia control.

$$P_{\mathrm{m}} - P_{\mathrm{e}} = J\omega_0 \frac{\mathrm{d}\omega}{\mathrm{d}t} \tag{3}$$

$$\omega = \frac{\mathrm{d}\vartheta}{\mathrm{d}t} \tag{4}$$

Here, P_{m} is the mechanical power, P_{e} is the electrical power, ω_0 is the nominal angular frequency, ω is the output angular frequency, ϑ is the rotation angle, and J is the total moment of inertia of the rotor mass.

Fig. 5 shows a simplified block diagram for a synthetic electrical inertia control system. As illustrated, ESS are needed along the grid-forming control to provide the necessary synthetic electrical inertia. This shows that ESS are an important factor in the energy transition and will play a key role in the future. Energy storage systems will provide inertia for local grid stability as well as other necessary AS, such as steady state voltage control, fast reactive current injections, short-circuit current, black start capability, and island operation capability [79].

Moreover, ESS will also need to compensate for weather and seasonal fluctuations in the power supply from IRES, specially from wind and solar power. For all the previous reasons, ESS are becoming increasingly important. New possibilities for medium and long-term ESS with sufficient storage capacity and flexibility, in accordance with the respective requirements, are needed to meet the growing demand from IRES. Low-head PHS system is a power generation system and serves at the same time as an ESS. This makes the integration of PHS (low-head or high-head) via grid-forming controlled converter a vitally important milestone of the energy transition in order to provide the necessary storage capacity needed for grid stability and flexibility. The grid integration of low-head PHS via a grid-forming, controlled converter will not only be of great significance for countries with flat topographies such as Denmark, Belgium, and the Netherlands. It will also be essential for countries with a high share of offshore wind energy as these could enable the concept of energy islands.

5. Electric machines and control for low-head pumped hydro storage

5.1. Electric machines

In traditional high-head, high-power PHS, synchronous machines with excitation winding and direct grid connection are used. However, doubly-fed induction machines have been adopted in Europe since 2006 for lower power applications. Doubly-fed induction machines are coupled to a partially rated converter with rotor winding to increase the operating range, which increases turbine efficiency at lower speeds [82]. As can be seen from Eq. (2), RPT operation at low head and high power reduces the nominal rotational speed for a fixed specific speed. Therefore, the power take-off (PTO) in low-head PHS needs to be designed to operate at high efficiency for low rotational speeds. Furthermore, variable speed RPTs require a highly efficient PTO over a wide operating range. Doubly-fed induction machines with a gearbox were the classical choice for such low-speed applications. However, with the recent decrease in cost of power electronics, permanent magnet synchronous machines (PMSM) with a fully rated converter are opted for instead [83–90]. Advantages include a high power density, high efficiency, and controllability over a wide operating range [91,92]. Furthermore, PMSMs with a large pole number avert the use of reduction gearing, which reduces energy losses and increases reliability [93,94]. However, the increased cost of permanent magnets (PM) and converter losses limits its application for high-power installations.

A more recent development in PMSMs is the axial flux PMSM (AF-PMSM), which has a magnetic flux direction parallel to the axis of rotation, in contrast to their radial counterparts. These disc-type machines have a high diameter-to-length ratio, can accommodate high pole numbers, and are suitable for high-torque low-speed applications [95–97]. They have a higher power density and use less core iron, leading to a lower weight [96,98,99], which in turn results in a higher torque-to-weight ratio. The possible topologies are single-stator single-rotor (SSSR), double-stator single-rotor (DSSR), or single-stator double-rotor (SSDR). Furthermore, different concepts can be differentiated on the use of surface mounted or interior PMs, slotted or slotless armature, presence or absence of stator core, concentrated or distributed windings, etc. [100].

Single-stator single-rotor topologies [101] are simple in design and compact. However, there is a strong imbalanced axial force between the stator and rotor. Therefore, the rotor disc width needs to be increased to avoid twisting [96]. Double-stator single-rotor topologies [102] are a valuable alternative to SSDR topologies. Double-stator single-rotor uses fewer PMs, but experiences more copper losses due to poor winding utilisation [96]. A DSSR machine with integrated permanent magnets has a high power-to-inertia ratio, since the rotor disc serves no magnetic purpose and is eliminated [100]. The reduced inertia is a significant benefit in a grid-supporting low-head PHS. In a slotted stator AF-PMSM, cogging torque results from the interaction between the PMs and the stator slots. This undesired torque can be significantly reduced by changing the angle between both stators [103]. However, this also reduces power output. Finally, SSDR is deemed the most favourable AF-PMSM topology. Next to decreased copper losses, the use of a stator yoke and the corresponding iron losses can be averted. This can be achieved by using a north–south PM arrangement of the rotors. Then, the flux path is completely axial, obviating the magnetic function of the yoke. The single-stator double-rotor topology has already been adopted in wind and tidal turbine applications [104,105]. An SSDR with coreless stator maximises efficiency, while averting cogging torque and torque ripple [106–108]. Since the flux path is axial, grain-oriented material – which has greater magnetic permeability in one direction – can be used in the stator slots. This results in significantly lower iron losses compared to non-oriented material [109], while reducing PM use compared to coreless alternatives [100].

Especially in high-voltage electric machines, the vast majority of occurring faults are stator faults, followed by rotor and bearing faults [110]. Therefore, AF-PMSMs with concentrated windings can offer a significant advantage by adopting a Modular Machine Drive (MMD) design. If a fault arises in one of the stator windings, the MMD can compensate this with the other modules and remain functional albeit the maximum power is reduced [111,112]. This fault-tolerant design improves the reliability of the electric machine, which is a considerable advantage for a low-head PHS system providing grid support. The reliability can be further increased by means of condition monitoring techniques and fault or anomaly detection methods [113,114]. Thanks to the drastic increase in computational power in the past years (both local and in the cloud), these techniques have become more data-driven, relying on, e.g., machine learning [115,116], including artificial neural networks [117], support vector machines [118], and deep learning [119,120]. The use of digital twins for predictive maintenance of mechanical components [121] or the full drivetrain [122] shows promising results and offer a perspective for the future of condition monitoring [123]. These techniques can be applied on the electric machine, and in extension on the whole drivetrain. Current, voltage, magnetic flux, speed, temperature, and vibration signals can be captured on the electric machine and serve as inputs for the condition monitoring system.

It can be concluded that the PMSM is currently the most sensible electric machine technology for modern low-head PHS due to its high efficiency and direct-drive capability, although the use of rare earth materials is a drawback. The principles of axial flux design, modularity for fault tolerance and data-driven condition monitoring are likely to play a role in the further improvement of the PMSM.

5.2. Torque and speed control

In variable speed PHS, the machine speed is altered to reach a power setpoint as fast and precise as possible, both in pump and turbine mode. Therefore, the machine torque must be precisely controlled. Field oriented control (FOC) is a vector control method that has been widely used in low-head micro-hydropower installations [83–89]. The main advantage is an independent control of the machine torque, and thus, highly dynamic performance. This is necessary in PHS to quickly react to changes to the rapidly fluctuating grid frequency. The general principle of FOC is to regulate the i_d and i_q currents in the rotating reference frame. The electrical dynamics of a PMSM can be modelled by Eqs. (5) and (6). Here, $\Omega_e \Psi_{PM}$ is the back-EMF of the permanent magnets. R is the stator resistance. L_q and L_d are the q and d axis inductances, respectively. $\Omega_e L i$ is the armature reaction EMF, through which the q and d schemes are coupled.

$$v_d = R\, i_d + L_d \frac{di_d}{dt} - \Omega_e L_q i_q \tag{5}$$

$$v_q = R\, i_q + L_q \frac{di_q}{dt} + \Omega_e (L_d i_d + \Psi_{PM}) \tag{6}$$

By regulating the d and q axis currents, the torque can be regulated as shown in the general torque Eq. (7) of the PMSM.

$$T = p\, \frac{3}{2} \left[\Psi_{PM} i_q + (L_d - L_q) i_d i_q \right] \tag{7}$$

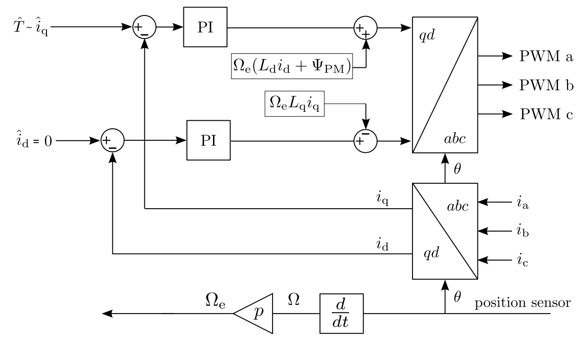

Fig. 6. Decoupled field oriented control of a PMSM with estimated back-EMF feedforward.

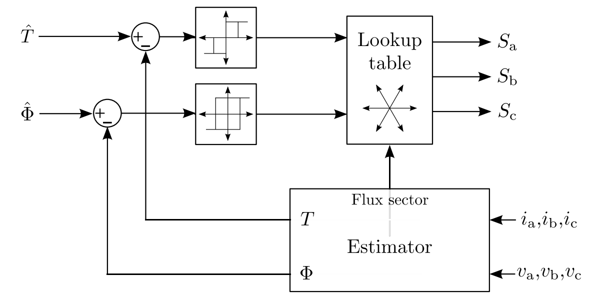

Fig. 7. Control schematic of DTC.

Here, p is the pole pair number and Ψ_{PM} is the constant flux of the permanent magnets. Fig. 6 shows the control scheme of a field oriented controlled PMSM. On the bottom right, the stator currents are measured and transformed to the rotating q, d reference frame. These signals are compared with the setpoints on the left and controlled by two PI controllers. These controllers determine the duty ratios resulting in the Pulse-Width Modulated (PWM) signals for the converter. In FOC, $\hat{i}_d$ is set to 0. Eq. (7) shows that the machine torque is directly proportional to i_q, resulting in a highly dynamic control. To achieve decoupled control of both currents, the coupling terms in Eq. (7) are used as a feedforward. Furthermore, a back-EMF estimator can be implemented in the q current control.

Although FOC is highly dynamic and easy to implement, setting $i_d = 0$ is not the most efficient way to reach a desired torque setpoint for a PMSM with saliency, like an interior magnet PMSM. Therefore, maximum torque per ampere (MTPA) control can reduce copper losses and increase overall efficiency in low-head hydropower applications. The MTPA accomplishes this by minimising $i_s = \sqrt{i_q^2 + i_d^2}$ for every torque setpoint [124]. Applications with interior magnet PMSMs in wind turbines found a reduction in Joule losses (up to 4.2%), while maintaining a dynamic response to changing torque setpoints [124, 125].

The position sensor plays a critical role in FOC. However, a position sensor is costly and its signal can contain noise. Therefore, saliency-based sensorless rotor position estimators [88,89,126,127] are proposed for low-power systems, since they can increase reliability and reduce cost [89]. For low rotational speed runners, as in low-head PHS, the saliency-based approach is the most suitable [89]. Here, a high pulse frequency is injected, while the current response, which depends on the rotor magnetic flux position, is observed.

Active distribution rejection control (ADRC) is used in torque and speed control to account for known and unknown electrical, hydraulical, or mechanical disturbances in the system, increasing performance and robustness. Guo et al. [84] applies a first order ADRC for a PMSM in a hydropower application, where the known disturbances are mechanical friction and hydraulic torque. A second order state observer is used to estimate the rotational speed and hydraulic torque. ADCR is especially useful in low-head high-power PHS, since any change in the system tubes has a significant influence on the head losses, because of the high flow rate at low head.

Direct torque control (DTC) is an alternative control method to FOC. In DTC, the electromagnetic torque and stator flux are controlled by switching between a discrete number of stator voltage vectors, which in turn form the stator flux vector interacting with the rotor flux. Based on the torque and flux linkage reference and the current flux vector position, a lookup table is consulted to select the optimal voltage vector. If e.g. the torque must be increased, a voltage vector is selected so that the angle between stator and rotor flux is increased. Fig. 7 visualises the control schematic. To find the torque and stator flux, an estimator based on phase voltages and currents is used (bottom). These estimated values are compared to torque and flux setpoints. Hysteresis controllers then determine the proper voltage vector from a lookup table, resulting in the switching signals. Direct torque control has a slightly better torque response compared to FOC and does not require a position sensor [128,129]. However, DTC relies on an accurate estimator. Especially at low speeds, an estimator based on phase voltages and currents cannot accurately estimate the stator flux [130] which makes it less suitable for low-head PHS. Although some improved estimator algorithms have been studied [130], this drawback is best averted by using a position sensor in the estimator. Disadvantages of DTC include variable switching frequency, high harmonic current distortion, and torque ripple [128,129,131]. To achieve a smoother dynamic response and thus less torque and flux ripple, space vector modulation (SVM) is used instead of the lookup table [128,129,132].

5.3. Power control

In the power control of low-head PHS, the goal is to reach a power setpoint as fast and efficiently as possible. Three main control parameters are determined: the pump/turbine rotational speed Ω; the inlet vane angle α; and the blade pitch β. An RPT with only Ω as control parameter is defined as a non-regulated RPT. A single- and double-regulated RPT further include, respectively inlet vane control, and inlet vane and blade pitch control. In low-head PHS, a regulated RPT is recommended, because it allows the RPT to be operated at high efficiency in a large operating range of heads, flow rate, and power setpoint.

5.3.1. Maximum power point tracking algorithms

Maximum power point tracking (MPPT)-based algorithms are used to find the optimal speed setpoint for a certain power setpoint in turbine mode. In a low-head turbine, this power setpoint is the maximum available power, hence the name MPPT. In grid-supporting PHS, this may not be the case, as the power setpoints depend on grid frequency. Therefore, adjustments need to be made to the existing algorithms. The MPPT algorithms can be divided into direct and indirect methods. Direct MPPT algorithms are based on iterative extremum-seeking control algorithms. These algorithms require limited knowledge of the system, but are inherently slow due to their iterative behaviour, making them less suitable for grid-supporting PHS. However, they can still be used in storage systems with lower dynamic requirements because of their simplicity. Indirect methods are based on a model of the system, making them more dynamic but less flexible. Most of the existing MPPT control methods rely on flow rate measurement. However, a flow rate sensor is costly and has a certain error. In low-head RPTs, the accuracy can further decrease due to a non-uniform flow, a short intake, and high turbulence [133]. To evade these drawbacks, Borkowski and Dariusz [90] presented a flow rate estimator. The estimator is based on an artificial neural network (ANN), which is trained by experimental data.

Among direct MPPT control methods, the perturb and observe algorithm has been investigated for non-regulated low-head turbines. The principle operation consists of altering or perturbing the rotational speed Ω, i.e. accelerating or decelerating, and analysing the change in output power P, measured at the electric machine or converter. If the power has increased, the sign of $\mathrm{d}\Omega$ is maintained and the procedure continues. Otherwise, $\mathrm{d}\Omega$ is reversed [83]. Eq. (8) shows how the speed setpoint $\hat{\Omega}$ is altered after each iteration. Note that $\delta(t)$ implies the sign of $\mathrm{d}\Omega$.

$$\hat{\Omega} = \int_{t_{k-1}}^{t_{k-1}+T_s} K\delta(t)\ \mathrm{d}t \tag{8}$$

$$\delta(t) = \mathrm{sgn}(P_k - P_{k-1})\ \mathrm{sgn}(\Omega_k - \Omega_{k-1}) \tag{9}$$

Inherent to this method is that the system will still perturb Ω when the MPP is reached, resulting in an oscillation around the MPP. Step size K is an adaptive value that increases when the power is continuously rising and decreases when the power is fluctuating [83]. However, the dynamic behaviour of this method is not optimal. If K is too low after oscillations and the MPP shifts, the dynamic response is poor. To allow both dynamic response and minimal power fluctuation around the MPP, K can be taken proportional to the power gradient $\frac{\Delta P}{\Delta \Omega}$ [134]. Due to the parabolic nature of the turbine characteristics, K is high when far away from the MPP and gradually decreases when the MPP is neared. Note that using this gradient-based step size cannot be used to reach a lower power setpoint $\hat{P}$. However, the step size here can be proportional to $|\hat{P} - P|$. In wind turbine applications, fuzzy logic is recently used to find the value of K, where the perturbed variable is the generator voltage, which is proportional to the generator speed [135–137].

Gradient descent control is a direct maximum efficiency point tracking (MEPT) algorithm that allows multiple control variables, opposed to the perturb and observe algorithm. However, to derive the efficiency, an accurate flow sensor is necessary, which was discussed to be a challenge in low-head PHS systems [133]. On every operating point, the control variables are incremented with the direction of their partial derivatives of efficiency at the current operating point, multiplied by a step size k [138]. In Eq. (10), α is the vane opening and β is the blade pitch.

$$\Delta\alpha = k\frac{\partial\eta}{\partial\alpha} \qquad \Delta\beta = k\frac{\partial\eta}{\partial\beta} \qquad \Delta\Omega = k\frac{\partial\eta}{\partial\Omega} \tag{10}$$

If the time constants of the control parameters are known, k can be chosen differently for each control parameter. Furthermore, k can be adaptive and defined by a line search algorithm at every iteration [139]. Although this control algorithm shows great potential, any disturbances on the gradient estimation due to measurement error or mutual influence between control parameters has a great impact on the convergence [138]. Therefore, a moving average filter and a Kalman filter can, respectively, be used to increase robustness [90,140]. Furthermore, Borkowski [90] accounts for the time delay of flow rate settlement after a change in turbine control parameter further reduce risk of a non-converging control.

Indirect MPPT algorithms rely on prior knowledge of the system in order to determine the optimal torque or speed reference to achieve a power setpoint. Recently, this system knowledge is mostly captured in the form of empirical equations, hill charts, or lookup tables, which are derived from measurements or numerical analysis like computational fluid dynamics. Márquez et al. [141] derived an empirical formula for a propeller turbine, which is a modified Kaplan turbine, designed for low-heads and low flow rates. Eq. (11) relates the non-regulated turbine efficiency to flow rate and turbine speed.

$$\eta_h(\Omega, Q) = 3.33\ Q\left[\frac{1}{2}\left(\frac{90}{\lambda_i} + Q + 0.78\right)e^{\frac{-50}{\lambda_i}}\right] \tag{11}$$

$$\lambda_i = \left[\frac{1}{(\lambda + 0.089)} - 0.0035\right]^{-1}, \quad \lambda = \frac{R A \Omega}{Q}$$

Although this model can be used in low-head control models, it is important to note that flow rate Q is a function of head and rotational speed $Q = f(H, \Omega)$ for a non-regulated RPT. Therefore, changing Ω will affect flow rate Q as well. Zhang et al. [142] proposes a polynomial empirical equation for the efficiency of a turbine $\eta_h(\Omega, Q)$, where the coefficients can be derived from experimental data. Borkowski and Dariusz [143] used an ANN to compose and validate an efficiency equation $\eta_h(\Omega, Q)$ together with a flow rate characteristic $Q(\Omega, \alpha)$ for a regulated turbine. The control system based on these characteristics requires no flow rate sensing. However, the Q characterisation is for a constant head and the flow rate is approximated by a linear function of speed. This limits its application under varying head at low rotational speeds.

Similarly, ANN has also been used to form lookup tables [144]. Lookup tables can be constructed over a large operating range during on-site measurements or by using an existing dataset. Pérez-Diaz and Fraile-Ardanuy [144] use two ANNs to train the head and efficiency for input parameters Q, Ω, and α. A possible application of the resulting lookup tables is to find reference $\hat{\Omega}$ and $\hat{\alpha}$ to reach the optimal efficiency for a given head. In this control system, no flow sensor is necessary, thus reducing cost and increasing reliability, especially for low-head systems.

Hill charts define the relation between flow rate Q, rotational speed Ω, inlet vane angle α, and efficiency η for a constant head H. Therefore, if Ω and α are known, Q and η can be read from the graph. Furthermore, α and η are plotted versus the unitary rotational speed Ω_{11} and unitary flow rate Q_{11} in Eq. (12), making hill charts scalable for different heads. However, in a real system, the losses $H_L(Q)$ have to be taken into account, making it difficult to estimate the net head across the turbine without a flow rate sensor. Especially in a low-head high-power system, where the flow rate is high, these losses have a significant influence on the efficiency.

$$\Omega_{11} = \frac{\Omega\ D}{\sqrt{H}}, \quad Q_{11} = \frac{Q}{D^2\sqrt{H}} \tag{12}$$

Q_{11} and Ω_{11} can also be compensated when the Reynolds number of the real system differs from the design [145]. Fraile-Ardanuy et al. [146] applied a hill chart to a control system in order to find the optimal efficiency speed for given α and measured Q. For a reduced-scale RPT [147], a lookup table is trained based on measurements. The lookup table is used to find $\hat{\Omega}$ for given measured H and $\hat{P}$. However, the speed is controlled by α, while it was shown in the paper that $Q_{11} = f(\alpha, \Omega)$. However, the proposed control system is promising for low-head hydropower if both Ω and α are controlled separately. Then, the RPT could be controlled to reach $\hat{P}$ at the highest efficiency for a certain measured H.

One drawback of using turbine characteristics is that the electrical machine and converter losses are not included. Therefore, the overall MPP may differ from the turbine MPP [87]. De Kooning et al. [148] found that the MPP displacement in wind turbines was greater for low wind and thus lower rotational speeds. In direct MPPT methods, these losses are included if the power is measured on the converter side. Another drawback of indirect MPPT methods is that they do not account for system performance deterioration over a long time period. However, reinforcement learning, as proposed for wind turbines [149,150], can solve this problem at the cost of a higher real computational intensity.

5.3.2. Model predictive control

An important factor in RPT operation and control that is often overlooked in traditional MPPT strategies is the transient effect of the water supply system caused by a control action. The transient flow equations are described in Section 6.1. Fang et al. [151] stated that increasing the control action magnitude actually decreased the output power, while the settling and maximum turbine pressure deviation increased. Therefore, it can be seen how using an MPPT control that does not account for these effects can have poor dynamic behaviour when applied to a real system. In some studies on MPPT control, the water inertia time T_w is incorporated as a time delay on the control action [90] or as an extra mechanical inertia on the RPT [152]. However, this does not fully capture the transient effects. Therefore, model predictive control (MPC) is applied to PHS systems [153–155]. In MPC, a detailed model of the full PHS system, including hydraulic transients, losses, and an RPT model, are used. Based on a certain operating state setpoint, an internal optimisation algorithm simulates control actions and observes the predicted outcomes of the model. The outcomes are then given a cost value based on the power response. These predictions are made for multiple future time samples. Each time sample, this process is repeated. Therefore, MPC is an accurate control method that can work on complex systems, at the cost of a significantly high computational intensity. Furthermore, MPC can also incorporate system constraints, such as maximum pressure deviation and mechanical rate limits. Chaoshun et al. [153] proposed using a nonlinear MPC, which includes the elastic water hammer effect in a high-head PHS plant. Liang et al. [154] used MPC to define the optimal switching time between pump and turbine mode for a multi-RPT PHS plant. However, these studies did not include pressure constraints, which are especially important in systems with long pipelines. The MPC for a 40 metre PHS plant by Mennemann et al. [155] included this effect. MPC is currently mostly investigated for high-head PHS. However, the benefits of adapting MPC for low-head PHS could be substantial, because of the potentially increased influence of transient effects, as described in Section 6.1. For a dynamic system providing frequency support, the MPC's computational intensity increases even further, which might slow down the optimisation algorithm. However, with the recent advancements made in parallel computing with, e.g., multi-core processors (CPUs) and many-core processors such as graphical processing units (GPUs), the MPC process can be accelerated [156], making it suitable for complex dynamic systems like low-head PHS.

6. Modelling of low-head systems

The overall objective of developing a model of a given system is to have a representation of the real world. Since such a model will always be a simplified depiction, it is crucial to weigh which aspects are essential and what should be left out or simplified. In the case of numerical models, this also helps to improve performance and reduce the computational resources necessary. At the end, a well formulated model allows to predict the behaviour of a system to a greater extent and wider scenarios than experiments and interpolating empirical data. These predictions are crucial in developing such systems to understand performance and dynamics, aid optimisation, and can be required for accurate control during operation. The mathematical models are typically derived from first principles, such as balance equations of mass, energy, or momentum, but can also be based on phenomenological or empirical observations or a mixture of both.

Models for high-head PHS are comprehensive and well researched while attention to low-head PHS applications has been limited. Fundamentally, the same approaches can be used. There are, however, differences in the relevance of individual model components. From a hydrodynamic point of view, the major difference is a shift towards higher flow and reduced head for a given power. The increase in the mass flow rate of water may cause the system to be more prone to water hammer effects. Cavitation is a further effect to consider when choosing model components for a low-head scenario. Reaction turbines, such as Francis or Kaplan turbines that are suitable for medium- and low-head applications, are considered more susceptible to the effect [157].

The different relation between flow and head also affects turbomachinery and power take-off. The shift to a higher flow and lower pressure at the machine side closer to the upper reservoir typically results in lower angular velocity and higher torque at the runner and motor-generator. This is due to an increased runner tip speed as a consequence of enlarged machines. In combination with the likely use of variable speed control which may cause even lower speeds at off-design operation points, this may, for example, not just affect the choice of motor-generator architecture but could also affect the drivetrain losses. When choosing modelling approaches for individual system components, considering these characteristics specific for low-head PHS helps to cover the relevant aspects while also optimising performance.

6.1. Hydrodynamics

One of the most common approaches in PHS is to model the penstock as a rigid conduit in addition to the consideration of water being an incompressible fluid. A widespread approach making these assumptions is based on the net force on the body of water which can be given through both the rate of change of momentum and the differences in pressure head to obtain the change in time of the volumetric flow rate as shown in Eq. (13) [158–160].

$$L\frac{\mathrm{d}Q}{\mathrm{d}t} = \left(H - H_{\mathrm{T}} - H_{\mathrm{L}}\right) Ag \tag{13}$$

Here, Q is the volumetric flow rate through the conduit and turbine, H is the head over the body of water, H_{T} is the turbine head, H_{L} represents the head losses within the conduit, g is the gravitational acceleration, A is the conduit cross-sectional area, and L is the conduit length. The turbine head can be obtained either from empirical data or physical models as a function of both its rotational speed and flow rate, while the major and minor head losses are typically represented through well known hydraulic models, such as the Darcy–Weisbach formulation in combination with the Colebrook equation [50]. To complete the conduit component of the system model, these equations are typically coupled with equations relating to a governor, such as a gate or guide vanes and mechanical power of the turbine as given in Eq. (1).

Using the above mentioned combination of ordinary differential and algebraic equations to model the water column as a rigid body is one the simplest methods to cover the system dynamics. However, to accurately depict transients in the system, such as travelling pressure waves, an approach using coupled partial differential equations considering compressibility and elasticity is required [161]. This could be particularly relevant in applications where enlarged mass flow rates of water are subject to sudden changes of flow rates and heads, such as low-head PHS. A commonly used 1-D approach considering these effects uses the so-called, water hammer equations. These relate pressure head and water velocity as a function of position and time as shown in Eqs. (14) and (15) [162,163].

$$\frac{\partial H}{\partial t} = -U\frac{\partial H}{\partial x} - \frac{a^2}{g}\frac{\partial U}{\partial x} \tag{14}$$

$$\frac{\partial U}{\partial t} = -U\frac{\partial U}{\partial x} - \frac{fU|U|}{2D} - g\frac{\partial H}{\partial x} \tag{15}$$

Here we have H as the pressure head, U as water velocity, a as the pressure wave velocity, g as gravitational acceleration, D as the conduit diameter, and f as friction factor. If appropriate, simplifications can be made neglecting velocity head or friction losses. The set of partial differential equations can be solved either directly or by transforming it first into a series of ordinary differential equations.

Comparisons of similar approaches have shown that treating the conduit as rigid results in a reduction in computational resources necessary and hence, decreased simulation time. However, if the underlying scenario requires, higher accuracy can be achieved when considering elasticity and compressibility effects [163,164].

Aside from travelling pressure waves, another effect that may be of higher relevance in a low-head high-flow system is cavitation. The inception of cavitation is dependent on the amount and type of particles in the water allowing for nuclei to sustain [165]. Low-head PHS is a promising candidate for seawater applications in coastal regions. In such, breaking waves mixing particles from the seabed with the salty water could increase the risk for cavitation to occur. Its likelihood is also increased when pump-turbines work at off-design conditions as a consequence of variable speed operation.

This formation of vapour bubbles occurs when the local reference pressure in the fluid reaches its vapour pressure. Fundamental numerical estimates for the likelihood of cavitation occurrence use different forms of a dimensionless cavitation parameter, such as *Thoma's* cavitation number shown in Eq. (16) [166].

$$\sigma = \frac{p_r - p_v(T)}{\Delta p} \tag{16}$$

Such cavitation numbers characterise how close the local reference pressure is to the vapour pressure of the fluid. It is calculated from the reference pressure p_r, the vapour pressure at the given temperature $p_v(T)$, and the characteristic system pressure difference Δp. Approaches using various forms of the cavitation number have shown widespread use in a variety of hydrodynamic applications. It has been found, however, that studies giving too much emphasis to it, result in poor repeatability and inconsistency between them. This is due to a wide variety of definitions of the cavitation number as well as the neglect of other factors, such as the influence of geometry, flow velocity, or fluid temperature [167]. More accurate approaches typically include representations of the dynamics of the vapour bubble cluster. While computationally more intensive, these allow to model growth and collapse of the nuclei based on the Rayleigh–Plesset equation derived from the conservation of mass allowing to solve for the time-dependent vapour bubble radius [168,169].

6.2. Power take-off

Variable speed operation of PHS does not just enable to work at improved efficiency under varying conditions but also improves the capability to provide AS. When modelling newly developed low-head PHS systems, this should be considered. For variable speed systems in low-head PHS as well as related and comparable wind power generation, a variety of power take-off architectures and controls are available. Commonly used are models representing doubly-fed induction or permanent magnet synchronous motor-generators, respectively, in combination with drivetrain models of the change in angular velocity based on torque balance and inertia [161,170,171]. To model the drivetrain, the simplest model consider a lumped rigid body approach with a rigid shaft such that all rotating masses and hence rotational inertias can be added together, leading to Eq. (17).

$$J\frac{d\omega}{dt} = \tau_h - \tau_g - D_f\omega \tag{17}$$

This ordinary differential equation relates the change in angular velocity ω and rotational mass moment of inertia of the system J to the balance of hydraulic torque τ_h, generator torque τ_g, as well as friction typically represented as a viscous damping torque $D_f\omega$. Typical implementations modelling the electrical dynamics of motor-generators use space-vector representation with the d-q frame of reference. An example for such an approach for a PMSM can be found in Eqs. (5) and (6) described in Section 5.2.

A further point of interest to modelling the PTO of low-head PHS in combination with variable speed operation is a potential shift to higher Joule and reduced iron losses. The changing loss characteristics could affect control and supporting models when tracking optimal operating point to extract maximum power as shown on the example of wind turbines [172]. Effects that are potentially less relevant for low-head applications are the influence of cogging torque and resulting speed ripple. The shift towards lower angular velocity and increased torque for a given power means cogging will be a smaller fraction of the total torque. Additionally, larger diameters of the rotating mass lead to increased rotational inertia. An increase here correlates with a reduction in speed ripple [173]. This becomes clear when including a cogging torque in Eq. (17).

7. Conclusion

Due to the rapid rise of intermittent renewable energy sources, penetration levels will exceed what can be compensated for by alternative stability measures, and large-scale integration of energy storage will become imperative. This increase in demand for short- and long-term balancing and the provision of ancillary services will contribute to novel systems turning into cost-effective solutions. While pumped hydro storage is a promising candidate to improve grid stability, its limitations in deployability call for a conceptual adaptation. Shifting the operating range from traditional high-head towards low-head applications could pave the way to utilise PHS in regions where so far it had not been feasible. Further technological advancements can significantly contribute to enhancing its capability to improve grid stability while also making it cost competitive. Based on the lack of research on low-head PHS, this review discusses challenges and the potential of low-head PHS while giving an overview of pumped storage technologies and their applicability to low-head applications. The main outcomes are the following:

- In a low-head context, the choice of pump-turbine design is highly dependent on the flow rate of the system. Axial flow pump-turbines, with variable speed drives, are the most suitable solution for high flow rates which leads to higher power outputs. On the other hand, other designs, such as Archimedes screw or rotary positive displacement configurations, can be beneficial at lower flow rates and micro- or small-scale locations.
- The discussion on grid integration has shown that, to compensate for an increase in intermittent generation and a reduction in spinning reserves, a combination of grid-forming control alongside bulk energy storage is necessary. To ensure grid stability, such systems will need to provide synthetic inertia next to other ancillary services, namely steady state voltage control, fast reactive current injections, short circuit currents, black start, and island operation capability.
- For the power take-off, axial flux PMSMs are the most promising electric machines for low-head PHS due to their high efficiency, high power density, and suitability for high-torque-low-speed operation. The machine torque can be controlled to achieve a speed setpoint by either field oriented control or direct torque control, with the latter having a slightly better torque response if a position sensor is used, but increasing torque ripple. Active distribution rejection control can be used to complement the torque and speed control, increasing performance and robustness. To derive the speed setpoint, MPPT algorithms based on RPT models are suitable for low-head PHS because of their short response time and steady power output. However, it is important to include the whole system with its losses to have precise control. Model predictive control is a computationally intense control method that can account for transient effects in complex systems, making it a valuable option for low-head PHS.
- When modelling low-head PHS, the same fundamental approaches of traditional PHS can be used. However, the change in system characteristics being a shift to larger masses of water and reduced head requires more attention on certain model components. Modelling hydrodynamics in more detail allows to cover transients such as water hammer and estimate the risk of cavitation. Paying further attention to changing motor-generator dynamics can help to accurately predict performance and improve control.

There are considerable opportunities for further research to improve low-head pumped storage technology and facilitate economic viability. Firstly, a detailed economic analysis incorporating a predicted increase in revenue from energy arbitrage and the provision of AS combined with improved control strategies optimised for these may serve as a further proof of concept. Additionally, modelling and simulation efforts integrating the proposed components and analysing performance on a system level can help to estimate technical potential for round-trip efficiencies, mode-switching times, and power ramp rates. Finally, a step from such theoretical results to prototyping and implementation would attract attention of stakeholders and pave the way for large-scale deployment. With these steps taken, low-head PHS has the potential to be a significant facilitator for the ongoing energy transition.

Declaration of competing interest

The authors declare that they have no known competing financial interests or personal relationships that could have appeared to influence the work reported in this paper.

Acknowledgements

This research is part of a project that has received funding from the European Union's Horizon 2020 research and innovation programme under grant agreement No. 883553. The authors would like to thank the International Hydropower Association for providing us with Fig. 2.

References

[1] International Energy Agency. Global energy review 2021. Global energy review 2020. 2021, p. 1–36.
[2] International Energy Agency. Renewables information - overview (2020 edition). IEA Stat 2020;497.
[3] Jülch V. Comparison of electricity storage options using levelized cost of storage (LCOS) method. Appl Energy 2016;183:1594–606.
[4] Barnhart CJ, Benson SM. On the importance of reducing the energetic and material demands of electrical energy storage. Energy Environ Sci 2013;6(4):1083–92.
[5] REN21. Renewables 2021 global status report. 2021.
[6] Rehman S, Al-Hadhrami LM, Alam MM. Pumped hydro energy storage system: A technological review. Renew Sustain Energy Rev 2015;44:586–98.
[7] Richter W, Vereide K, Pikl FG, Pummer E. Economic and sustainable energy transition enabled by pumped-storage hydropower plants. 2020, p. 1–10.
[8] IHA. Hydropower status report 2020. International Hydropower Association; 2020, p. 1–44.
[9] Rogner M, Law S. Pumped storage tracking tool. International Hydropower Association; 2021.
[10] Koohi-Fayegh S, Rosen MA. A review of energy storage types, applications and recent developments. J Energy Storage 2020;27:101047.
[11] Wissenschaftliche Dienste des Deutschen Bundestages. Vor- und Nachteile verschiedener Energiespeichersysteme. 2014.
[12] Statkraft Markets GmbH. Speicherlösungen für den Energiemarkt der Zukunft.
[13] Ren J, Ren X. Sustainability ranking of energy storage technologies under uncertainties. J Clean Prod 2018;170:1387–98.
[14] Stocks M, Stocks R, Lu B, Cheng C, Blakers A. Global atlas of closed-loop pumped hydro energy storage. Joule 2021;5(1):270–84.
[15] Blakers A, Stocks M, Lu B, Cheng C. A review of pumped hydro energy storage. Prog Energy 2021;3(2):022003.
[16] Barbour E, Wilson IA, Radcliffe J, Ding Y, Li Y. A review of pumped hydro energy storage development in significant international electricity markets. Renew Sustain Energy Rev 2016;61:421–32.
[17] Joseph A, Chelliah TR, Lee SS, Lee K-b. Reliability of variable speed pumped-storage plant. Electronics 2018;7(10).
[18] Ardizzon G, Cavazzini G, Pavesi G. A new generation of small hydro and pumped-hydro power plants: Advances and future challenges. Renew Sustain Energy Rev 2014;31:746–61.
[19] Kougias I, Aggidis G, Avellan F, Deniz S, Lundin U, Moro A, et al. Analysis of emerging technologies in the hydropower sector. Renew Sustain Energy Rev 2019;113:109257.
[20] Javed MS, Zhong D, Ma T, Song A, Ahmed S. Hybrid pumped hydro and battery storage for renewable energy based power supply system. Appl Energy 2020;257(May 2019):114026.
[21] Bódis K, Monforti F, Szabó S. Could Europe have more mini hydro sites? A suitability analysis based on continentally harmonized geographical and hydrological data. Renew Sustain Energy Rev 2014;37:794–808.
[22] Deane JP, Ó Gallachóir BP, McKeogh EJ. Techno-economic review of existing and new pumped hydro energy storage plant. Renew Sustain Energy Rev 2010;14(4):1293–302.
[23] Puchta M, Bard J, Dick C, Hau D, Krautkremer B, Thalemann F, et al. Development and testing of a novel offshore pumped storage concept for storing energy at sea - Stensea. J Energy Storage 2017;14:271–5.
[24] Pradhan A, Marence M, Franca MJ. The adoption of seawater pump storage hydropower systems increases the share of renewable energy production in small island developing states. Renew Energy 2021;177:448–60.
[25] Berrada A, Loudiyi K, Zorkani I. System design and economic performance of gravity energy storage. J Clean Prod 2017;156:317–26.
[26] Feltes J, Kazachkov Y, Gong B, Trouille B, Donalek P, Koritarov V, et al. Modeling ternary pumped storage units. 2013.
[27] Fisher RK, Koutník J, Meier L, Loose V, Engels K, Beyer T. A comparison of advanced pumped storage equipment drivers in the US and Europe. 2012.
[28] Nicolet C, Béguin A. Variable speed and ternary units to mitigate wind and solar intermittent production. 2014.
[29] Sterner M, Stadler I. Handbook of energy storage. 2019.
[30] European Environment Agency. EU Renewable electricity has reduced environmental pressures; targeted actions help further reduce impacts. 2021, p. 1–14.
[31] Foley AM, Leahy PG, Li K, McKeogh EJ, Morrison AP. A long-term analysis of pumped hydro storage to firm wind power. Appl Energy 2015;137(2015):638–48.
[32] Zakeri B, Syri S. Electrical energy storage systems: A comparative life cycle cost analysis. Renew Sustain Energy Rev 2015;42:569–96.
[33] Kougias I, Szabó S. Pumped hydroelectric storage utilization assessment: Forerunner of renewable energy integration or Trojan horse? Energy 2017;140:318–29.
[34] Hunt J, Byers E, Riahi K, Langan S. Comparison between seasonal pumped-storage and conventional reservoir dams from the water, energy and land nexus perspective. Energy Convers Manage 2018;166:385–401.
[35] McLean E, Kearney D. An evaluation of seawater pumped hydro storage for regulating the export of renewable energy to the national grid. Energy Procedia 2014;46:152–60.
[36] Okot DK. Review of small hydropower technology. Renew Sustain Energy Rev 2013;26:515–20.
[37] Loots I, Van Dijk M, Barta B, Van Vuuren SJ, Bhagwan JN. A review of low head hydropower technologies and applications in a South African context. Renew Sustain Energy Rev 2015;50(2015):1254–68.
[38] Hunt JD, Zakeri B, Lopes R, Barbosa PSF, Nascimento A, Castro NJd, et al. Existing and new arrangements of pumped-hydro storage plants. Renew Sustain Energy Rev 2020;129:109914.
[39] Vasudevan KR, Ramachandaramurthy VK, Venugopal G, Ekanayake JB, Tiong SK. Variable speed pumped hydro storage: A review of converters, controls and energy management strategies. Renew Sustain Energy Rev 2021;135:110156.
[40] Chapallaz JM, Eichenberger P, Fischer G. Manual on pumps used as turbines, Vol. 11. Deutsches Zentrum fur Entwicklungstechnologien GATE; 1992, p. 229.
[41] Dixon SL, Hall CA. Fluid mechanics and thermodynamics of turbomachinery. Seventh ed.. Butterworth-Heinemann; 2014.
[42] Stepanoff AJ. Centrifugal and axial flow pumps : theory, design and application. Wiley; 1948.
[43] Ak M, Kentel E, Kucukali S. A fuzzy logic tool to evaluate low-head hydropower technologies at the outlet of wastewater treatment plants. Renew Sustain Energy Rev 2017;68:727–37.
[44] Hogan TW, Cada GF, Amaral SV. The status of environmentally enhanced hydropower turbines. Fisheries 2014;39(4):164–72.
[45] Karassik IJ, Messina JP, Cooper P, Heald CC. Pump handbook, 4th ed.. New York: McGraw-Hill Education; 2008.
[46] Carravetta A, Derakhshan Houreh S, Ramos HM. Introduction. In: Pumps as turbines: fundamentals and applications. Springer Tracts in Mechanical Engineering, Cham: Springer International Publishing; 2018, p. 3–26.
[47] Bogenrieder W. 2.6. Pumped Storage power plants. In: Heinloth K, editor. Renewable energy, Vol. 3C. Springer-Verlag Berlin Heidelberg; 2006, p. 165–96.
[48] Breeze P. Chapter 8 - pumped storage hydropower. In: Breeze P, editor. Hydropower. Academic Press; 2018, p. 73–8.
[49] Morabito A, de Oliveira e Silva G, Hendrick P. Deriaz pump-turbine for pumped hydro energy storage and micro applications. J Energy Storage 2019;24:100788.
[50] White FM. Fluid mechanics, eighth edition. 2016.
[51] Braitsch W, Haas H. 2.7 Turbines for hydroelectric power. In: Heinloth K, editor. Renewable energy, Vol. 3C. Springer Berlin Heidelberg; 2006, p. 197–222.
[52] Novara D, McNabola A. A model for the extrapolation of the characteristic curves of pumps as Turbines from a datum best efficiency point. Energy Convers Manage 2018;174:1–7.
[53] Binama M, Su W-T, Li X-B, Li F-C, Wei X-Z, An S. Investigation on pump as turbine (PAT) technical aspects for micro hydropower schemes: A state-of-the-art review. Renew Sustain Energy Rev 2017;79:148–79.
[54] Delgado J, Andolfatto L, Covas DIC, Avellan F. Hill chart modelling using the Hermite polynomial chaos expansion for the performance prediction of pumps running as turbines. Energy Convers Manage 2019;187:578–92.
[55] Furukawa A, Shigemitsu T, Watanabe S. Performance test and flow measurement of contra-rotating axial flow pump. J Therm Sci 2007;16(1):7–13.

[56] Fahlbeck J, Nilsson H, Salehi S. Flow characteristics of preliminary shutdown and startup sequences for a model counter-rotating pump-turbine. Energies 2021;14(12):3593.

[57] Kim J-W, Suh J-W, Choi Y-S, Lee K-Y, Kanemoto T, Kim J-H. Optimized blade design of counter-rotating-type pump-turbine unit operating in pump and turbine modes. Int J Rotating Mach 2018.

[58] Kim J-H, Kasahara R, Kanemoto T, Miyaji T, Choi Y-S, Kim J-H, et al. Multi-objective optimization of a counterrotating type pump-turbine unit operated at turbine mode. Adv Mech Eng 2014;6:467235.

[59] Fahlbeck J, Nilsson H, Salehi S, Zangeneh M, Joseph M. Numerical analysis of an initial design of a counter-rotating pump-turbine. IOP Conf Series: Earth Environ Sci 2021;774(1):12066.

[60] YoosefDoost A, Lubitz WD. Archimedes screw turbines: A sustainable development solution for green and renewable energy generation—A review of potential and design procedures. Sustainability 2020;12(18):7352.

[61] Zhou D, Deng ZD. Ultra-low-head hydroelectric technology: A review. Renew Sustain Energy Rev 2017;78(May):23–30.

[62] Waters S, Aggidis GA. Over 2000 years in review: Revival of the archimedes screw from pump to turbine. Renew Sustain Energy Rev 2015;51:497–505.

[63] Sari MA, Badruzzaman M, Cherchi C, Swindle M, Ajami N, Jacangelo JG. Recent innovations and trends in in-conduit hydropower technologies and their applications in water distribution systems. J Environ Manage 2018;228:416–28.

[64] Krampe P, Ørke PR. Four-quadrant operation of rotary lobe pumps and regenerative throttling. In: Pump users international forum 2012, international rotating equipment conference 2012. 2012.

[65] Kurokawa J, Matsui J, Choi Y-D. Flow analysis in positive displacement micro-hydro turbine and development of low pulsation turbine. Int J Fluid Mach Syst 2008;1(1):76–85.

[66] Phommachanh D, Kurokawa J, Choi Y-D, Nakajima N. Development of a positive displacement micro-hydro turbine. Jsme Int J Series B-Fluids Therm Eng 2006;49:482–9.

[67] Sonawat A, Choi Y-S, Kim KM, Kim J-H. Parametric study on the effect of inlet and outlet pipe shape on the flow fluctuation characteristics associated with a positive displacement hydraulic turbine. Renew Energy 2021;163:1046–62.

[68] Sonawat A, Kim S-J, Yang H-M, Choi Y-S, Kim K-M, Lee Y-K, et al. Positive displacement turbine - a novel solution to the pressure differential control valve failure problem and energy utilization. Energy 2020;190:116400.

[69] Bocquel A, Janning J. Analysis of a 300 MW variable speed drive for pump-storage plant applications. In: 2005 european conference on power electronics and applications. 2005, p. 10 pp.–P.10.

[70] Javed MS, Ma T, Jurasz J, Amin MY. Solar and wind power generation systems with pumped hydro storage: Review and future perspectives. Renew Energy 2020;148:176–92.

[71] Jover MC. Optimal joint day-ahead energy and secondary regulation reserve scheduling of pumped-storage power plants operating with variable speed or in hydraulic short-circuit mode in the Iberian electricity market. (Ph.D. thesis), Technical University of Madrid; 2017.

[72] Next Kraftwerke GmbH. What are ancillary services?.

[73] Colas F, Qoria T, Guillaud X, Gruson F. Deliverable 3.5: Local control for GridForming converters: Experimental validation. tech. rep., 2019.

[74] Qudaih M, Engel B, Truijen D, Kooning J, Stockman K, Hoffstaedt J, et al. The contribution of low head pumped hydro storage to a successful energy transition. 2020.

[75] Siemens AG. Parallel compensation comprehensive solutions for safe and reliable grid operation. tech. rep., 2016.

[76] ENTSO-E. Synchronous condenser. ENTSO-E Technopedia 2021.

[77] Unruh P, Nuschke M, Strauß P, Welck F. Overview on grid-forming inverter control methods. Energies 2020;13(10).

[78] Laudahn S, Seidel J, Engel B, Bülo T, Premm D. Substitution of synchronous generator based instantaneous frequency control utilizing inverter-coupled DER. In: 2016 IEEE 7th international symposium on power electronics for distributed generation systems. 2016, p. 1–8.

[79] EU. DIrective (eu) 2019/944 of the European Parliament and of the council of 5 june 2019 on common rules for the internal market for electricity and amending directive 2012/27/EU. tech. rep., 2019.

[80] Kerdphol T, Watanabe M, Mitani Y, Phunpeng V. Applying virtual inertia control topology to SMES system for frequency stability improvement of low-inertia microgrids driven by high renewables. Energies 2019;12(20).

[81] Kerdphol T, Rahman FS, Mitani Y. Virtual inertia control application to enhance frequency stability of interconnected power systems with high renewable energy penetration. Energies 2018;11(4).

[82] Alizadeh Bidgoli M, Yang W, Ahmadian A. DFIM Versus synchronous machine for variable speed pumped storage hydropower plants: A comparative evaluation of technical performance. Renew Energy 2020;159:72–86.

[83] Belhadji L, Bacha S, Munteanu I, Rumeau A, Roye D. Adaptive MPPT applied to variable-speed microhydropower plant. IEEE Trans Energy Convers 2013;28(1):34–43.

[84] Guo B, Bacha S, Alamir M, Mohamed A, Boudinet C. LADRC Applied to variable speed micro-hydro plants: Experimental validation. Control Eng Pract 2019;85:290–8.

[85] Márquez JL, Molina MG, Pacas JM. Dynamic modeling, simulation and control design of an advanced micro-hydro power plant for distributed generation applications. Int J Hydrog Energy 2010;35(11):5772–7.

[86] Ducar I, Marinescu C. Increasing the efficiency of motor-pump systems using a vector controlled drive for PMSM application. In: 2014 international symposium on fundamentals of electrical engineering. 2014, p. 1–5.

[87] Iman-Eini H, Frey D, Bacha S, Boudinet C, Schanen J-L. Evaluation of loss effect on optimum operation of variable speed micro-hydropower energy conversion systems. Renew Energy 2019;131:1022–34.

[88] Abd El Maguid Ahmed W, Adel MM, Taha M, Saleh AA. PSO Technique applied to sensorless field-oriented control PMSM drive with discretized RL-fractional integral. Alex Eng J 2021;60(4):4029–40.

[89] Bonifacio J, Amann N, Kennel R. Silent low speed self-sensing strategy for permanent magnet synchronous machines based on subtractive filtering. In: 2017 brazilian power electronics conference. 2017, p. 1–6.

[90] Borkowski D. Maximum efficiency point tracking (MEPT) for variable speed small hydropower plant with neural network based estimation of turbine discharge. IEEE Trans Energy Convers 2017;32(3):1090–8.

[91] Sanchez AG, Molina MG, Lede AMR. Dynamic model of wind energy conversion systems with PMSG-based variable-speed wind turbines for power system studies. Int J Hydrog Energy 2012;37(13):10064–9.

[92] Tripathi SM, Tiwari AN, Singh D. Grid-integrated permanent magnet synchronous generator based wind energy conversion systems: A technology review. Renew Sustain Energy Rev 2015;51:1288–305.

[93] Dubrovskiy G, Peter S, Lappeen E-M, Mikerov A, Dzhankhotov V, Pyrhonen J. General comparison of direct and geared drives for control applications. In: 2014 16th european conference on power electronics and applications. 2014, p. 1–6.

[94] Touimi K, Benbouzid M, Tavner P. Tidal stream turbines: With or without a gearbox? Ocean Eng 2018;170:74–88.

[95] Cavagnino A, Lazzari M, Profumo F, Tenconi A. A comparison between the axial flux and the radial flux structures for PM synchronous motors. IEEE Trans Ind Appl 2002;38(6):1517–24.

[96] Gieras J, Wang R-J, Kamper M. Axial flux permanent magnet brushless machines. Springer; 2008, p. 55–6.

[97] Vansompel H, Sergeant P, Dupré L. Optimized design considering the mass influence of an axial flux permanent-magnet synchronous generator with concentrated pole windings. IEEE Trans Magn 2010;46(12):4101–7.

[98] Sitapati K, Krishnan R. Performance comparisons of radial and axial field, permanent-magnet, brushless machines. IEEE Trans Ind Appl 2001;37(5):1219–26.

[99] Pop AA, Jurca F, Oprea C, Chirca M, Breban S, Radulescu MM. Axial-flux vs. radial-flux permanent-magnet synchronous generators for micro-wind turbine application. In: 2013 15th european conference on power electronics and applications. 2013, p. 1–10.

[100] Kahourzade S, Mahmoudi A, Ping HW, Uddin MN. A comprehensive review of axial-flux permanent-magnet machines. Can J Electr Comput Eng 2014;37(1):19–33.

[101] Wirtayasa K, Irasari P, Kasim M, Widiyanto P, Hikmawan M. Design of an axial-flux permanent-magnet generator(AFPMG) 1 kw, 220 volt, 300 rpm, 1 phase for pico hydro power plants. In: 2017 international conference on sustainable energy engineering and application. 2017, p. 172–9.

[102] Djebarri S, Charpentier JF, Scuiller F, Benbouzid M. Design and performance analysis of double stator axial flux pm generator for rim driven marine current turbines. IEEE J Ocean Eng 2016;41(1):50–66.

[103] Mengesha S, Rajput S, Lineykin S, Averbukh M. The effects of cogging torque reduction in axial flux machines. Micromachines 2021;12:323.

[104] Laxminarayan SS, Singh M, Saifee AH, Mittal A. Design, modeling and simulation of variable speed axial flux permanent magnet wind generator. Sustain Energy Technol Assess 2017;19:114–24.

[105] Jin J, Charpentier JF, Tang T. Preliminary design of a TORUS type axial flux generator for direct-driven tidal current turbine. In: 2014 first international conference on green energy. 2014, p. 20–5.

[106] Anitha N, Bharanikumar R. Design and analysis of axial flux permanent magnet machine for wind power applications. In: 2019 international conference on power electronics applications and technology in present energy scenario. 2019, p. 1–4.

[107] El-Hasan TS. Development of axial flux permanent magnet generator for direct driven micro wind turbine. In: 2016 IEEE international conference on renewable energy research and applications. 2016, p. 169–72.

[108] Lok C, Balakrishnan V, T Subramaniam R. Implementation of hybrid pattern search–genetic algorithm into optimizing axial-flux permanent magnet coreless generator(AFPMG). Electr Eng 2017;99.

[109] Kowal D, Sergeant P, Dupre L, den Bossche A. Comparison of nonoriented and grain-oriented material in an axial flux permanent-magnet machine. IEEE Trans Magn 2010;46(2):279–85.
[110] He J, Somogyi C, Strandt A, Demerdash NAO. Diagnosis of stator winding short-circuit faults in an interior permanent magnet synchronous machine. In: 2014 IEEE energy conversion congress and exposition. 2014, p. 3125–30.
[111] Verkroost L, Vansompel H, Belie FD, Sergeant P. Distributed control strategies for modular permanent magnet synchronous machines taking into account mutual inductances. In: 2020 IEEE/ASME international conference on advanced intelligent mechatronics (aim), proceedings. IEEE; 2020, p. 66–71.
[112] Mohamed AHR, Vansompel H, Sergeant P. An integrated modular motor drive with shared cooling for axial flux motor drives. IEEE Trans Ind Electron 2020;1–10.
[113] Chen Y, Liang S, Li W, Liang H, Wang C. Faults and diagnosis methods of permanent magnet synchronous motors: A review. Appl Sci 2019;9(2116).
[114] Kudelina K, Asad B, Vaimann T, Rassõlkin A, Kallaste A, Khang HV. Methods of condition monitoring and fault detection for electrical machines. Energies 2021;14(22).
[115] Stetco A, Dinmohammadi F, Zhao X, Robu V, Flynn D, Barnes M, et al. Machine learning methods for wind turbine condition monitoring: A review. Renew Energy 2019;133:620–35.
[116] Lei Y, Yang B, Jiang X, Jia F, Li N, Nandi AK. Applications of machine learning to machine fault diagnosis: A review and roadmap. Mech Syst Signal Process 2020;138:106587.
[117] Lee H, Jeong H, Koo G, Ban J, Kim SW. Attention recurrent neural network-based severity estimation method for interturn short-circuit fault in permanent magnet synchronous machines. IEEE Trans Ind Electron 2021;68(4):3445–53.
[118] Ebrahimi BM, Faiz J. Feature extraction for short-circuit fault detection in permanent-magnet synchronous motors using stator-current monitoring. IEEE Trans Power Electron 2010;25(10):2673–82.
[119] Kao I-H, Wang W-J, Lai Y-H, Perng J-W. Analysis of permanent magnet synchronous motor fault diagnosis based on learning. IEEE Trans Instrum Meas 2019;68(2):310–24.
[120] Piedad EJ, Chen Y-T, Chang H-C, Kuo C-C. Frequency occurrence plot-based convolutional neural network for motor fault diagnosis. Electronics 2020;9(10).
[121] Liu Z, Chen W, Zhang C, Yang C, Chu H. Data super-network fault prediction model and maintenance strategy for mechanical product based on digital twin. IEEE Access 2019;7:177284–96.
[122] Rassõlkin A, Orosz T, Demidova GL, Kuts V, Rjabtšikov V, Vaimann T, et al. Implementation of digital twins for electrical energy conversion systems in selected case studies. Proc Est Acad Sci 2021;70(1):19–39.
[123] Falekas G, Karlis A. Digital twin in electrical machine control and predictive maintenance: State-of-the-art and future prospects. Energies 2021;14(18).
[124] Chowdhury MM, Haque ME, Saha S, Mahmud MA, Gargoom A, Oo AMT. An enhanced control scheme for an IPM synchronous generator based wind turbine with MTPA trajectory and maximum power extraction. IEEE Trans Energy Convers 2018;33(2):556–66.
[125] Demirkov B. Improved wind turbine control using maximum torque per ampere control strategy taking into account the magnetic saturation. Electrotech Electron (E+E) 2019;54(2):26–34.
[126] Salem WAA, Osman GF, Arfa SH. Adaptive neuro-fuzzy inference system based field oriented control of PMSM speed estimation. In: 2018 twentieth international middle east power systems conference. 2018, p. 626–31.
[127] Scicluna K, Staines CS, Raute R. Sensorless position control of a PMSM for steer-by-wire applications. In: 2016 international conference on control, decision and information technologies. 2016, p. 46–51.
[128] Gupta NP, Gupta P. Performance analysis of direct torque control of PMSM drive using SVPWM - inverter. In: 2012 IEEE 5th india international conference on power electronics. 2012, p. 1–6.
[129] El Mourabit Y, Derouich A, El Ghzizal A, El Ouanjli N, Zamzoum O. DTC-SVM Control for permanent magnet synchronous generator based variable speed wind turbine. Int J Power Electron Drive Syst 2017;8(4):1732–43.
[130] Foo G, Rahman MF. Sensorless direct torque and flux-controlled IPM synchronous motor drive at very low speed without signal injection. IEEE Trans Ind Electron 2010;57(1):395–403.
[131] Beng GFH. Sensorless direct torque and flux control of interior permanent magnet synchronous motors at very low speeds including standstill. (Ph.D. thesis), The University of New South Wales; 2010.
[132] Mesloub H, Boumaaraf R, Benchouia MT, Goléa A, Goléa N, Srairi K. Comparative study of conventional DTC and DTC-svm based control of PMSM motor — Simulation and experimental results. Math Comput Simul 2020;167:296–307.
[133] Staubli T, Abgottspon A. Discharge measurement in low head hydro power plants. In: 2017 international conference on energy and environment. 2017, p. 226–30.
[134] Krishnakumar R. V, Vigna KR, Gomathi V, Ekanayake JB, Tiong SK. Modelling and simulation of variable speed pico hydel energy storage system for microgrid applications. J Energy Storage 2019;24:100808.
[135] Mozafarpoor-Khoshrodi S-H, Shahgholian G. Improvement of perturb and observe method for maximum power point tracking in wind energy conversion system using fuzzy controller. Energy Equip Syst 2016;4(2):111–22.
[136] Putri R, Pujiantara M, Priyadi A, Ise T, Purnomo M. Maximum power extraction improvement using sensorless controller based on adaptive perturb and observe algorithm for PMSG wind turbine application. IET Electr Power Appl. 2018;12(4):455–62.
[137] Shahi A, Bhattacharjee C. A study analysis of fuzzy based p&o MPPT scheme in PMSG based wind turbine. In: 2018 technologies for smart-city energy security and power. 2018, p. 1–4.
[138] Borghetti A, Naldi G, Paolone M, Alberti M. Maximum efficiency point tracking for adjustable-speed small hydro power plant. 2008, p. 1–7.
[139] Chao R-M, Ko S-H, Lin H-K, Wang I-K. Evaluation of a distributed photovoltaic system in grid-connected and standalone applications by different MPPT algorithms. Energies 2018;11(6).
[140] Atta KT, Johansson A, Cervantes MJ, Gustafsson T. Phasor extremum seeking and its application in kaplan turbine control. In: 2014 IEEE conference on control applications. 2014, p. 298–303.
[141] Márquez JL, Molina MG, Pacas JM. Dynamic modeling, simulation and control design of an advanced micro-hydro power plant for distributed generation applications. Int J Hydrog Energy 2010;35(11):5772–7.
[142] Zhang J, Leontidis V, Dazin A, Tounzi A, Delarue P, Caignaert G, et al. Canal lock variable speed hydropower turbine design and control. IET Renew Power Gener 2018;12(14):1698–707.
[143] Borkowski D. Analytical model of small hydropower plant working at variable speed. IEEE Trans Energy Convers 2018;33(4):1886–94.
[144] Pérez-Diaz JI, Fraile-Ardanuy J. Neural networks for optimal operation of a run-of-river adjustable speed hydro power plant with axial-flow propeller turbine. In: 16th mediterranean conference on control and automation congress centre. 2008, p. 309–14.
[145] Heckelsmueller G. Application of variable speed operation on francis turbines. IngenierÍA E InvestigaciÓN 2015;35:12–6.
[146] Fraile-Ardanuy J, Wilhelmi JR, Fraile-Mora J, Pérez-Díaz J, Sarasúa I. Speed control of run-of-river variable speed hydro plants. 2006.
[147] Pannatier Y, Kawkabani B, Nicolet C, Simond J-J, Schwery A, Allenbach P. Investigation of control strategies for variable-speed pump-turbine units by using a simplified model of the converters. IEEE Trans Ind Electron 2010;57(9):3039–49.
[148] De Kooning JDM, Vandoorn TL, Van de Vyver J, Meersman B, Vandevelde L. Displacement of the maximum power point caused by losses in wind turbine systems. Renew Energy 2016;85:273–80.
[149] Wei C, Zhang Z, Qiao W, Qu L. Reinforcement-learning-based intelligent maximum power point tracking control for wind energy conversion systems. IEEE Trans Ind Electron 2015;62(10):6360–70.
[150] Tomin N, Kurbatsky V, Guliyev H. Intelligent control of a wind turbine based on reinforcement learning. In: 2019 16th conference on electrical machines, drives and power systems. 2019, p. 1–6.
[151] Fang H, Chen L, Dlakavu N, Shen Z. Basic modeling and simulation tool for analysis of hydraulic transients in hydroelectric power plants. IEEE Trans Energy Convers 2008;23(3):834–41.
[152] Borkowski D, Majdak M. Small hydropower plants with variable speed operation—An optimal operation curve determination. Energies 2020;13(23).
[153] Li C, Mao Y, Yang J, Wang Z, Xu Y. A nonlinear generalized predictive control for pumped storage unit. Renew Energy 2017;114:945–59.
[154] Liang L, Hou Y, Hill DJ. GPU-Based enumeration model predictive control of pumped storage to enhance operational flexibility. IEEE Trans Smart Grid 2019;10(5):5223–33.
[155] Mennemann J-F, Marko L, Schmidt J, Kemmetmüller W, Kugi A. Nonlinear model predictive control of a variable-speed pumped-storage power plant. IEEE Trans Control Syst Technol 2021;29(2):645–60.
[156] Abughalieh K, Alawneh S. A survey of parallel implementations for model predictive control. IEEE Access 2019;1.
[157] Kumar P, Saini RP. Study of cavitation in hydro turbines-A review. Renew Sustain Energy Rev 2010;14(1):374–83.
[158] Mover, Working Group Prime and Supply, Energy. Hydraulic turbine and turbine control models for system dynamic studies. IEEE Trans Power Syst 1992;7(1):167–79.
[159] Berrada A, Loudiyi K, Garde R. Dynamic modeling of gravity energy storage coupled with a PV energy plant. Energy 2017;134:323–35.
[160] Jaeger ED, Janssens N, Malfliet B, Van De Meulebroeke FV. Hydro turbine model for system dynamic studies. IEEE Trans Power Syst 1994;9(4):1709–15.
[161] Mohanpurkar M, Ouroua A, Hovsapian R, Luo Y, Singh M, Muljadi E, et al. Real-time co-simulation of adjustable-speed pumped storage hydro for transient stability analysis. Electr Power Syst Res 2018;154:276–86.
[162] Sharma JD, Kumar A. Development and implementation of non- linear hydro turbine model with elastic effect of water column and surge tank. Int J Electr Electron Res 2014;2(4):234–43.

[163] Taniguchi H, Nagao T, Higasa H. Development of a pumped-storage power station model for power system stability study. Electr Eng Japan 1992;112(3):50–62.
[164] Vytvytsky L, Lie B. Comparison of elastic vs. inelastic penstock model using OpenModelica. In: Proceedings Of the 58th conference on simulation and modelling, Vol. 138. reykjavik, iceland; 2017, p. 20–8, september 25th – 27th, 2017.
[165] Kuiper G. Chapter 3 physics of cavitation : GAS CONTENT. Cavitation Ship Propuls 2010;9–79.
[166] Franc J-P, Michel J-M. Fundamentals of cavitation. 2005.
[167] Šarc A, Stepišnik-Perdih T, Petkovšek M, Dular M. The issue of cavitation number value in studies of water treatment by hydrodynamic cavitation. Ultrason Sonochemistry 2017;34:51–9.
[168] Carlton J. Marine propellers and propulsion. 2019.
[169] Kumar PS, Pandit AB. Modeling hydrodynamic cavitation. Chem Eng Technol 1999;22:1017–27.
[170] Papaefthimiou S, Papathanassiou S. Modeling of a variable speed wind turbine with synchronous generator. In: European wind energy conference and exhibition 2009, Vol. 7. EWEC 2009, (ISlE):IEEE; 2009, p. 4439–48.
[171] Wu F, Zhang XP, Ju P. Modeling and control of the wind turbine with the direct drive permanent magnet generator integrated to power grid. In: 3rd international conference on deregulation and restructuring and power technologies. (April):2008, p. 57–60.
[172] De Kooning JDM, Vandoorn TL, de Vyver J, Meersman B, Vandevelde L. Displacement of the maximum power point caused by losses in wind turbine systems. Renew Energy 2016;85:273–80.
[173] Kral C, Pirker F, Pascoli G. The impact of inertia on rotor faults effects theoretical aspects of the vienna monitoring method. In: 2007 IEEE international symposium on diagnostics for electric machines, power electronics and drives, Vol.23. (4):2007, p. 77–82.